8-19-2016

Investigating Unit Stream Power and Drainage Capture in the Upper Dajia River, Taiwan using Geomorphic Indices

Lindsey C. Belliveau
University of Connecticut, lindsey.belliveau@uconn.edu

Investigating Unit Stream Power and Drainage Capture in the Upper Dajia River, Taiwan using Geomorphic Indices

Lindsey Constance Belliveau
B.S., Eastern Connecticut State University, 2014

A Thesis
Submitted in Partial Fulfillment of the
Requirements for the Degree of
Master of Science
At the
University of Connecticut
2016

APPROVAL PAGE

Masters of Science Thesis

Investigating Unit Stream Power and Drainage Capture in the Upper Dajia River, Taiwan using Geomorphic Indices

Presented by
Lindsey Constance Belliveau, B.S.

Major Advisor: _____
William B. Ouimet

Associate Advisor: _____
Timothy Byrne

Associate Advisor: _____
Anjali Fernandes

University of Connecticut

2016

ACKNOWLEDGEMENTS

Throughout the process of creating this thesis, I have learned a lot about being a scientific researcher. From the beginning, gained experience piecing my interest and excitement about Taiwan's geology into interesting and pursuable scientific questions that could be purposed to funding organizations, such as NSF and GSA. This took a great deal of critical analysis and research techniques that were new to me, including critical literature review, use of digital programs and analyses, data interpretation, and scientific writing. The foremost technique that I worked on improving from start to finish was finding eloquent and provocative ways to present the "so what" factor of my research to both broad and focused audiences.

With learning new techniques came many challenges that I had to overcome, the most difficult being the writing process. Scientific writing has always been a struggle of mine due to my tendency to "meander" around my words. I owe a lot of my learning and improvement to the critiques and coaching of Dr. Tim Byrne, who set aside multiple meetings on his personal time in Taiwan to guide me away from my struggles. Another challenge that I faced was access to funding. Since this project was from scratch, there was absolutely no funding for it. Dr. William Ouimet taught me a lot about the grant application process to receive the crucial funds for getting to Taiwan for the necessary data acquisition and field work. Due to his guidance, I was able to be awarded an NSF/Taiwan MOST Eastern Asia and Pacific Summer Internship fellowship that provided both travel and living expenses that allowed me to spend three months abroad at Academia Sinica, Taiwan's premier research institute.

The next challenge that I faced was the actual design of the project itself. Since I initially did not know what data I would have access to or the amount of field work that could

be done, I flew into Taiwan with a completely blank slate. Dr. Yu-Chang Chan was an excellent mentor in teaching me how use available resources to create a scientific question that was able to be explored in the three months I spent abroad. Although the original scope of the project changed throughout my career as a graduate student, his guidance was absolutely crucial to help me learn how to avoid research that is too broad and focus on an attainable scope.

I would like to give additional thanks to my lab groups in both Taiwan and at UConn, as they provided useful insight towards my research as well as advice for different techniques to approach challenges brought forth in the research process. I would also like to thank Chung Huang, Han-Cheng Yu, and Wendy Chang for helping with my daily life in Taiwan to make my transition there as smooth as possible during the three months that I lived there. I would like to thank Matthew Tran for coding assistance in Python and Matlab as well as for being a supportive boyfriend when I was away for three months on an opposite time zone and during the times that I was under a lot of stress and pressure and had to cancel dates or work through our time spent together on weekends. I would also like to thank my brother and mother for providing excellent support as well.

Foremost I owe all that I have learned, and hence produced, to the guidance and mentoring of my advisors: Dr. William Ouimet, Dr. Tim Byrne, and Dr. Anjali Fernandes. They have helped guide me into becoming the researcher that I now am and I plan to continue working with them in my future endeavors, some of which have already been started.

Table of Contents

CHAPTER ONE: INTRODUCTION AND PURPOSE

Taiwan is one of the most geomorphically and tectonically active regions in the world and is prone to intense erosion and mass-wasting due to its steep topography, large earthquakes, and frequent typhoons, resulting in river incision rates as high as 5–12 mm yr^{-1}, and decadal erosion rates averaging 15 mm yr^{-1}. These intense incision rates are likely related to the coupling of the westward propagation of the Taiwan thrust belt and its extreme climate (Dadson et al., 2003).

River incision into bedrock has strong control on overall topographic evolution. Therefore to further investigate topographic evolution, a rivers capability to incise can be modeled using normalized steepness index (k_{sn}; $m^{-0.9}$) and unit stream power (Watt/m^2). For an example, mass-wasting of valley walls often impacts a channel's ability to incise because the debris can dam a channel, lowering incision capacity upstream and increasing it downstream, thus altering physical morphology of the reach.

This study investigates the origin and evolution of complex channel morphology, terraces, and river capture using GIS analyses and field studies along a ~30km stretch of the Upper Dajia River, which flows between the Hsüehshan and Central Ranges of Taiwan. Evidence of river capture of the Dajia provides support for the dynamic interactions between river incision and mass-wasting in channels within steep, rapidly uplifting and evolving mountain belts.

CHAPTER TWO: BACKGROUND

2.1 TAIWAN GEOLOGY AND CLIMATE:

2.1.1 Tectonic Setting

The island of Taiwan is the result of the collision of the oceanic Philippine Sea Plate at ~7 – 8 cm/yr (Figure 1a) in the northwest direction with the continental Eurasian Plate (e.g. Dadson et al., 2003; Shyu et al., 2007; Gourley et al., 2007). This collision causes Taiwan's elongate shape with a north-south trend. As seen in Figure 1a, most of the major physical features tend to be parallel to this trend, including geological structures such as faults and folds, and topographic features including many rivers in the mountains. The collision originated ~5 Ma years ago when the Philippine Sea Plate collided with the Eurasian Plate (e.g. Tseng, 1990).

Observation of modern tectonics of the region may provide evidence towards the complexity of the Taiwan's tectonics, as shown in Figure 2. Examples of this exist in the rapidly uplifting mountains of Taiwan and the active spreading of the Okinawa trough in the Yilan Plain that causes an increase in surface area as well as subsidence in the plain. (e.g. Figures 1a, Figure 2) (Ching et al., 2000; Lin et al., 2010).

2.1.2 Geologic Setting of Taiwan

Taiwan can be divided into 6 major geologic providences (Figure 1a) (e.g. Gourley et al., 2007; Ching, et al., 2011). The mountains of Taiwan can be further divided into two subgroups with unique litho-tectonic characteristics – the Central (or Backbone) Range and the Hsüehshan Range. The Hsüehshan Range is the outer litho-tectonic belt composed of carbonaceous sandstone interbedded with in slate and Phyllite, and is commonly observed in anticlinal and synclinal folds separated by normal faults (e.g. Lee et al., 1997). The Backbone Range consists of mostly Miocene Lushan

and Eocene Pilushan Formations (slate and phyllite). The Western Foothills of the Central Range primarily consist of Late Cenozoic (Oligocene and Pleistocene) clastic deposits consisting of sediment transported from the Central Range that have undergone a much lower grade of metamorphism than the mountains. Primary lithology includes including sandstones, siltstones, and shale.

2.1.3 Climate in Taiwan

Taiwan has a subtropical climate that experiences warm, humid conditions as well as frequent precipitation, primarily from an average 3-5 typhoons per year that deliver an average precipitation of 2.5m yr^{-1} (Dadson et al., 2003). Tropical Rainfall Measuring Mission (TRMM) data shows that highest precipitation occurs in the mountain ranges and the lowest occurs in the western lowlands and Longitudinal Valley (Bookhagen, 2014).

2.2: RIVERS IN TAIWAN:

Rivers in Taiwan originate as mixed bedrock-alluvial channels in mountainous headwaters and transition to primarily alluvial channels in the eastern and western lowlands, with their mouths draining into the Philippine Sea or the Taiwan Strait. These rivers are rapidly incising in their headwaters due to intense precipitation and steep topography that increase flow velocities. These headwaters may experience incision rates as high as 5-12 mm yr^{-1} (Dadson et al., 2003). Conversely, these rivers are also subject to periods of intense deposition due to an abundance of mass wasting triggered extreme events such as earthquakes and typhoons. Some of these depositional events have been observed to cause as much as ~10m aggradation in some areas in a very short amount of time (e.g. Hsieh and Capart, 2013; Dadson et al 2003) (Figure 3). Some of these bursts of deposition may be more localized and related stochastic

disruptions such as an isolated landslide that blocks a channel. The cycle between intense deposition and subsequent incision in river channels allows for the mixed-bedrock-alluvial character of Taiwan's channels as well as the abundance of terraces that can be found alongside of them (Figures 4, 5).

2.3: TERRACE DEVELOPMENT

Terraces are flat, elevated features that are the remnants of paleo-channels and paleo-floodplains and are created when a fluvial system's base level elevation changes (Figures 4, 5). Base level changes can be due to tectonic disruptions, drainage capture, or sea level change (e.g. Anderson and Anderson, 2011; Ritter et al., 2010; Burbank and Anderson, 2013; Finnegan and Dietrich, 2011). These relict features can be used to estimate the past elevations, gradients, and geometries of channels. When correlated with one another, terraces can provide a window to the channel's past conditions, such as records of periods of increased aggradation or incision (e.g. Liew and Hsieh, 2000; Hsieh and Knuepfer, 2001; Hsieh and Capart, 2013). *Paired* terraces are found on both sides of a channel with equal elevation and gradient and tend to occur from allogenic influences that impact more than just one channel, such as region-wide base level change or climate fluctuations. *Unpaired* terraces occur at different elevations and may not occur on both sides of a channel. These terraces occur due to more isolated events, such as a blockage or local base level change, or by the individual mechanics within a system, such as individual meander evolution.

Many terraces in Taiwan are created following periods of increased aggradation. When a typhoon or earthquake related event triggers multiple landslides, a channel valley can rapidly fill, dramatically changing channel elevation and gradient. This

change in elevation and gradient may also be coupled with the steady uplift of the Central Range, as the filled channel is uplifted and continues to move further above base level. Previous research has correlated dated terraces throughout Taiwan and find signals of these bursts of aggradation in the past thousands of years. However it is difficult to decipher where tectonics or climate have a more significant impact on terrace creation (e.g. Liew and Hsieh, 2000; Hsieh and Knuepfer, 2001; Hsieh and Capart, 2013).

Some terraces, both in Taiwan and worldwide, can also develop independent of any specific triggers in response to the evolution of active meanders. Laterally incising meanders are not limited to broad, flat lowlands and can be found in steep mountainous, alluviated bedrock reaches (Finnegan et al., 2013; Finnegan and Dietrich, 2011*).* These unpaired terraces are much more localized and depend on the dynamics and characteristics of channel morphology (e.g. Bull, 1990; Finnegan and Dietrich, 2011). The sediment deposits in these steep alluviated channels can serve as tools that further intensify incision, unlike the finer-grained sediments that are transported in lowland meanders. Although not as common, these steep actively meandering channels have been found to both vertically and laterally incise simultaneously both in the field and through computational modeling (e.g. Finnegan and Dietrich, 2011; Finnegan, 2013). The inner banks, or point bars, will follow the outer cut banks, in lateral movement, much like meanders in lowlands. However, when coupled with intense vertical incision the lateral incision will leave multiple flights of terraces along the inner banks of the bend (Finnegan and Dietrich, 2011) (Figure 6).

2.4: Measured Width vs. Basic Scaling and Finnegan Scaling

Previous studies discuss the strong correlation between drainage area and channel width (e.g. Leopold and Maddock, 1953; Flint, 1974). Using this correlation, scaling relationships have been created to be used as a proxy when measured widths are not available. This allowed for a standard relationship (Leopold and Maddock, 1953; Flint, 1974) to be developed followed by an improved scaling method by Finnegan et al. (2005) which will be referred to in this study as "Basic Scaling" and "Finnegan Scaling", respectively. The produced widths are referred to as Basic Width (Equation 1; W_b) and Finnegan Width (Equation 2; W_f).

$$W_b = A^{0.5} * C \quad (1)$$

The variable *C* in this method refers to individual coefficients used to expand or contract the relationship to better reflect the patterns of the measured widths. Drainage area, is represented as *A*. The Finnegan method adds slope as in variable that influences channel width:

$$W_f = (A^{3/8} * S^{-3/16}) * C \quad (2)$$

Longitudinal slope is represented as *S.* Scaled widths were derived for every 100th point along the channel to gain a better representative difference in *S*. However, this scale as formatted to previous studies alone did not reflect a strong correlation in this study, so it was adjusted (W_{fB}):

$$W_{fB} = (A^{1/2} * S^{-1/4}) * C \quad (3)$$

2.5 Modeling Incision Capability along a Channel (Unit Stream Power and k_{SN})

The incision capability of a channel is dependent on a number of geomorphic incises, primarily drainage area, channel width, and the longitudinal slope of the channel (e.g. Flint, 1974; Yanites et al., 2010). Drainage area is a major control on a river's ability to incise as it increases flow volume, thus impacting the amount of mechanical work that it can do (e.g. Hack, 1957; Flint, 1974; Leopold et al., 1997; Anderson and Anderson, 2010; Ritter et al., 2011). This correlation produces a positive linear relationship between drainage area and incision capability.

Most fluvial profiles are thus well-described by a power-law relationship based on of shear-stress driven incision processes found between local channel gradient, k_s, and contributing drainage area, A, (e.g. Hack, 1957; Flint 1974; Snyder et al., 2000) raised to concavity index (θ), or longitudinal change in the slope of a channel, defined by Equation 4 (e.g. Tarboton et al., 1991.; Sklar and Dietrich, 1998):

$$S = k_s A^{-\theta} \qquad (4)$$

k_s is a coefficient used in the measure of channel gradient, referred to as the channel steepness (e.g. Whipple & Tucker, 1999; Snyder et al., 2000) which can be defined as:

$$k_s = (U/K)^{1/n} \qquad (5)$$

where U is uplift rate relative to a fixed base level, K is a coefficient of erodibility (such as lithology, climate, etc), and n is a constant that relates to hydraulic geometry, basin hydraulics, and erosion processes (Howard et al.,1994; Whipple and Tucker, 1999; Whipple et al., 2000; Kirby and Whipple, 2001) that is derived from the river profile evolution equation:

$$dz/dx = U(x,f) - KA^mS^n \quad (6)$$

In studies such as this one, this value gets considered a coefficient because these factors can be considered consistent in such a localized area. Concavity index (θ) can be found by using Equation 7, where m and n are constants that relate to erosion:

$$\theta = m/n \quad (7)$$

Although it is often difficult to use field measurements to determine m and n, this ratio has been found to be independent of erosion process (Whipple and Tucker 1999; Kirby and Whipple, 2001) and is often easier to estimate (Seidl and Dietrich, 1992; Whipple et al., 2007). Both theoretical and empirical considerations and data find average θ values range from 0.3 to 0.6 (e.g. Hack, 1957; Flint 1974, Whipple and Tucker, 1999; Snyder, et al., 2000), but some values as high as 1.1 have been found (Skylar and Dietrich, 1998). Θ can only be used in Equation 4 when conditions of K, U, m, and n can be considered constant throughout the study area (Kirby and Whipple, 2001). k_{sn} is a normalized steepness index so all the channels can be compared to one another (Kirby and Ouimet, 2011; Wobus et al., 2006; Snyder et al. 2000).

The assumption of a liner relationship with drainage area becomes complicated when the longitudinal slope along a channel is considered. Slope alters the acceleration of flow, impacting incision rate and altering the amount of work it can do (e.g. Yanites, et al., 2010). When the slope along individual reaches differ, incision capability may differ greatly from what was predicted using drainage area alone. These differences in slope can result from stochastic autogenic factors (e.g. individual landslides, channel avulsions) or wider reaching allogenic factors (e.g. tectonic activity, swarms of mass-

wasting). A normalized steepness index (k_{sn}) provides a metric of incision capability as it incorporates both slope (steepness) and drainage area along a channel.

Channel width variation further complicates the interpretation of incision capability as it has direct impact on the overall shear stress exerted by the channel (e.g. Whipple and Tucker, 1999). Study of fluid dynamics indicates that water can do more work when it is under more pressure. One way to change this pressure is to change the width that the water flows through. A decrease in width will constrict flow and increase its power. High stream power values most commonly occur in narrow, steep, scoured reaches like bedrock gorges, while low stream power values tend occur in broad aggrading valleys (Yanites et al., 2011; Whipple and Tucker, 1999; Kirby and Whipple, 2001). Width can be altered by the same controls that affect steepness but may also be more inherent from the landscape such as general topography fluctuations (Finnegan et al., 2004).

The work that is done by water flowing in a channel is known as unit stream power, defined as the rate of energy expended on the channel (Howard and Kerby, 1983; Whipple and Tucker, 1999). Unit stream power can be considered the best proxy to analyze incision capability because it considers physical properties of the rock, drainage area, longitudinal slope, and channel width and is thus considered the (e.g. Whipple and Tucker, 1999; Kirby and Whipple, 2001). The k_{sn} model can be considered a simplified form of the stream power because it does not consider channel width as an independent variable. Unit stream power is considered the most accurate proxy of incision capability each of these indices contribute important control over incision capability. This can be found using the following equation:

$$\omega = \rho\, g\, Q\, S / W \qquad (8)$$

where gravitational acceleration (*g),* density of water (*ρ*), discharge (*Q*), and slope (*S*) and then further dividing the product by channel width (*W*). When discharge is unavailable for a region, as is the case in this study, it can be substituted using:

$$Q = k_q A^c \qquad (9)$$

where k_q and *c* are dimensional constants that depend on runoff processes, climate, basin topology, and return period of effective discharge (Whipple and Tucker, 1999) and *A* is drainage area. Since these are consistent for this local study, they have been assigned a value of 1.

Although both depend on drainage area and slope, k_{sn} is most sensitive to slope adjustments because it is a simplified form of the stream power model and does not consider channel width, which greatly varies in this area of Taiwan. Due to the added variable of width, unit stream power is more accurate to true variations in incision capability within a channel. k_{sn} is not considered less useful however, as it can provide insight towards variations that are more slope influenced, such as a tectonic uplift or lithology variation, limiting noise that width may bring forth.

In both cases of k_{sn} and unit stream power, changes in incision capability will alter the behavior, and thus morphology, of a channel. Channels with higher capability to incise will cut a landscape down and approach base level, while those with low capability will aggrade and decrease in gradient over time as they fill in with alluvium (e.g. Anderson and Anderson, 2010; Burbank and Anderson, 2011; Ritter et al., 2011). An imbalance of incision capability on opposite sides of a drainage divide will cause the

higher capacity watershed to erode into, or capture, the lower capacity one. A river that has lower incision capability cannot compete with one that has higher incision capability and will begin to lose drainage area. This capture will continue until channel geometries equalize at attain steady state, and morphology will not significantly change thereafter, should the system remain undisturbed (e.g. Willet et al., 2014). Some conditions however, such as constant tectonic alteration, may never allow steady state to be attained.

2.6: Upper Dajia Study area

The Upper Dajia watershed covers ~445 km^2 above Techi Reservoir in the northern region of Taiwan's Central Range Mountains (to the east) and Hsüehshan Mountains (west) (Figure 7c). Subtropical forest with some cropland is the primary land cover type in this region. The Upper Dajia River flows west-southwestward for ~35km before reaching the head of the ~1,120 acre Techi Reservoir (~45km to the dam itself) over ~1040m relief. The Techi Reservoir Dam is 180m high and 290m long and was completed in 1974 by the Taiwan Power company for hydroelectric power, irrigation and some flood control (Chu, 1961). The major tributaries to the Upper Dajia described in this study include: the Qijiawan River which flows due south for ~12km over 1340m relief, Hehuan River that flows northeast for ~39km over 1718m relief, Nanhu River which flows southwest for ~31km over 2049m relief, and Sijilang (13km; 1854m) Rivers (Figure 4c).

Based on the geologic map of Taiwan (Chen, 1984), the Upper Dajia area consists of three formations including, from west to east, the Chiayang, Meichi, and Lushan Formations. The presence of these formations have been confirmed in limited

localities (Chen, 1976; Lee et al., 1997), but detailed unit distribution is unknown in the area because it is unmapped at a quadrangle scale and Chen's map (1984) is extrapolated from quadrangles to the north and south. Based on this extrapolation, the Chiayang Formation is composed of slate and phyllite and is Oligocene to Miocene in age. The Meichi Formation is composed of thin meta-sandstone interbedded with slate and is Eocene to Oligocene in age (Chen, 1976). The Lushan Formation is composed of slate and phyllite and is Miocene in age (Chen, 1976; Lee et al., 1997) (Figure 7a). The Lishan Fault, recognized as the Niutou Fault to north and as the Meichi Fault to the south, likely traces through the area but has not been mapped.

Measurements acquired island-wide from 199 Continuous GPS (CGPS) and 1873 highway leveling stations from 2000 - 2008 can be used to characterize the modern vertical and horizontal displacement field in Taiwan (Ching et al., 2000; Lin et al., 2010). Studies show that this area is rapidly uplifting in present time much like it has in the past when compared to rates estimated from radiometric dates (Ching et al., 2000; Lin et al., 2010; Dadson et al., 2003). Figure 2 GPS data indicates that the Central Range is rotating clockwise while the Hsüehshan Range is not rotating (Lin et al., 2010), suggesting that the Upper Dajia is undergoing extension. This is consistent with dilatational strain calculated from the GPS, which is inconsistent with the high uplift rates based on the leveling data that suggests shortening and crustal thickening. This anomaly requires further investigation.

CHAPTER THREE: DATA AND METHODS

3.1: DATA- DIGITAL ELEVATION MODELS, AIR PHOTOS, AND GEOGRAPHIC INFORMATION SYSTEMS (GIS)

Study site selection was performed following island-wide reconnaissance of aerial imagery, a 40m Digital Elevation Model (DEM), and a 30m Shuttle Radar Topography Mission (SRTM) of Taiwan. Regions with abundant terraces and meanders and preliminary evidence of current/past landslide dams were selected in the Central Range. Once the Upper Dajia study area was selected, a 5m DEM provided by Academia Sinica was used for the rest of the analyses. Initial analysis began with general mapping using the 5m DEM and Geographic Information Systems (GIS) using slope maps, elevation maps, and aerial imagery. This included the mapping of terraces and channels as polygons, as well as locating geomorphic features of interest (i.e. active/abandoned meanders, captured channels, landslide dams). “Channel” (flooded-valley) polygons were created using the slope map and were used for channel width analysis and terraces for preliminary height-correlation as discussed later.

3.1.1: Documenting Channel Morphology

Terraces and channels were mapped by hand in ArcGIS using the DEM as polygons. These channel geometry polygons were then used with the *ChanGeom* Matlab algorithm (Fisher et al., 2014) in tandem with ArcGIS to generate points along the reach of the channels to calculate their estimated widths. The *ChanGeom* algorithm uses raster images generated from the geometry polygons to calculate the centerline of a channel, enabling it to calculate widths by counting the pixels to the left and right of the centerline (Fisher et al., 2013). These points could then be brought back into ArcGIS

and fit to the flow accumulation path using the Hydrology tools in the Spatial Analyst toolbox so they could be plotted along the true location of the channel's flow rather than the mathematical center of the polygons. This adjustment was important because the centerline points often did not fall into pixels in the rasters that contained data crucial to be used along many of the tools in later parts of the analysis.

ChanGeom is designed to rely on polygons generated from aerial imagery such as Google Earth. However, due to poor image quality and heavy vegetation in this region of Taiwan, flooded valley widths were extracted from the 5m DEM slope map and used instead (Figure 8). Flooded valley widths were classified as the areas along the banks with no significant change in cross-sectional elevation or slope. The use of flooded valley widths may lend occasional slight over-estimation, but will not be subject to the sporadic errors that would result from using poor imagery.

Longitudinal profiles were generated for the Upper Dajia River and its major tributaries – Qijiawan, Nanhu, Hehuan, Sijilang Rivers - by extracting elevations from the DEM using the points generated by *ChanGeom* (Figure 9). The profiles were also be further analyzed alongside the *Stream Profiler* Matlab algorithm for comparison (Whipple et al., 2007). *Stream Profiler* extracts river profiles from DEM data and analyzes k_{sn} and concavity index of specific study channels or all the channels in a region batched together. A standard concavity index (θ) of 0.45 was used for this batch process. The k_{sn} values that were calculated using this tool were assigned to each *ChanGeom* point to be used for later analysis.

Longitudinal slope was another geomorphic index that was assigned to each *ChanGeom* point. A Python algorithm was developed for this study to calculate the

longitudinal slope of each point set at an appropriate interval specified for the reach, primarily to avoid the result of a negative slope value. Intervals of ~100 points up and down stream of each point (200 points total) were used for all of the channels in this study except Qijiawan (150 points) and the Dajia (300 points). These slope values were used for unit stream power (ω) calculation.

Analysis of Longitudinal Channel Profiles

The mechanics of incision in fluvial systems can be used to understand the relation between channel gradients and "disturbances" such as rock uplift or lithology (e.g. Flint, 1974; Howard & Kerby 1983; Howard et al. 1994; Whipple & Tucker 1999, 2002; Tucker 2004). Longitudinal profiles can be used to analyze this interaction with the physical landscape. Identification of knickpoints, or abrupt changes in gradient, serve as indicators of impacts to the river system such as tectonics or variations in lithology because they correlate with areas where incision capability has been altered (e.g. Hack, 1973; Sklar and Dietrich, 1998; Kirby and Ouimet, 2011).

3.1.2: Terrace Mapping

Terraces were mapped in ArcGIS and then field checked (Figures 10, 11). In addition to terraces, relict features such as abandoned meanders and channels were also included in this analysis. Average elevations for terraces and relict features were calculated using the mapped terrace polygons and Zonal Statistics tool in the Spatial Analyst toolbox of ArcGIS. These average elevations were plotted along the longitudinal profiles for preliminary correlation based on the terrace height above the modern stream (Figures _).

3.2 Fieldwork

Fieldwork consisted of reconnaissance of a currently geomorphically unmapped region of Taiwan. The primary goal of this fieldwork was to identify materials in terrace cuts and outcrops and to preform field-checks on significant features identified in the DEM. Fieldwork also included efforts to find organic-based samples viable for ^{14}C dating of aggradational features, however none were found in the 2015 field season. The extent of fieldwork was determined by ease accessibility due to limitations brought forth by Typhoon Soudelor (August 8, 2015), which blocked roads due to mass-wasting and produced flood stages in the rivers.

3.3: Scaling of Channel Widths

Width is an important component a channel's incision capability and is a crucial part of the unit stream power model. In addition to these measured widths from *Changeom*, various width scalings, Basic and Finnegan scalings, were calculated to determine how the measured widths compare to those that would be predicted based off of the other indices that are important in the stream power model such as drainage area (A) and slope (S).

3.4: K_{SN} and Unit Stream Power Calculations

Unit Stream Power (ω) was calculated for every 100th point generated from the *ChanGeom* algorithm (Fisher et al., 2013) and was assigned to every point due to computational limitations. These unit stream power values will be later compared to the k_{sn} values that were generated by the previously mentioned *Stream Profiler* algorithm (Whipple et al., 2007).

CHAPTER FOUR: RESULTS

4.1 MORPHOLOGY

General physical characteristics of the channels were studied using DEMs including elevation, stream-wise distance, and drainage area. The 5 rivers in this study are characteristic of Taiwan's rivers in that they are alluviated bedrock channels with primarily cobble to bolder-sized deposition with occasional sandy patches. Although geomorphic mapping is still in progress, many of the mapped terraces were field-confirmed as strath or fill-capped strath terraces. Abandoned channels and meanders are mapped alongside the terraces also seen in Figures 10, 11 and are later described in the discussion section (Chapter 5).

4.1.1 Longitudinal Profile:

The longitudinal profiles of the Dajia and its tributary channel are seen in Figure 9. These profiles can be used to locate knickpoints that indicate areas for potential increased incision capability (later discussed, Figure 15), general channel concavity/gradient, and overall channel patterns.

4.1.2 Terraces

Terraces and relict features can be seen on the map in Figures 10, 11. For the convenience of mapping, five groups of terraces are shown based on their relative elevation above the modern channels. Terraces that less than 5m above the stream may serve as a floodplain in extreme events and are characterized as *low terraces* (shown in yellow on the map; Figures 10, 11). Terraces that are too high to be reactivated during extreme events a referred to as *major terraces.* The major terraces are classified in 20m increments to show potential height correlations. Figure 11 shows an example of a major strath terrace located in the southern part of the study area.

4.1.3 Channel Width

Comparison of the various widths can be used to determine significant deviations in channel width from how it would be expected to behave according to controlling indices determined in previous studies such as drainage area and slope (e.g. Leopold and Maddock, 1953; Flint, 1974; Finnegan et al., 2005; Fisher et al., 2012; Kirby and Ouimet, 2011) (i.e. Figures 12, 13).

4.2 INCISION CAPABILITY - K_{SN} AND UNIT STREAM POWER

Once the basic morphologic indices of the system such as longitudinal slope, width, and drainage area are documented, proxies for understanding incision capability can be derived (e.g. Whipple et al., 2006, Yanites et al., 2010; Yanites and Tucker, 2010). k_{sn} and unit stream power were mapped side-by-side for comparison along the map in Figure 14 as well as plotted in graphs for each of the channels like the one shown in Figure 15 that show normalized comparison between the two incision potential values**.**

When both k_{sn} and unit stream power are analyzed, most of the channels in this study area reflect expected incision capability for this type of topography. The channel headwaters have a higher incision capability than their confluence with the main channel. However, the main channel (Upper Dajia) itself does not fit this pattern - there are no high k_{sn} or unit stream power values present in the headwaters and the entire channel has low or moderate low incision capability (shown in blue in Figure 14).

CHAPTER FIVE: DISCUSSION

5.1 INTERPRETATION OF PHYSICAL MORPHOLOGIES

Channel evolution can be investigated by investigating past channel gradients, elevations, and incisional/aggradational patterns. Such patterns can be found by observing current interactions between processes and morphological features. This section discusses the abundant physical evidence that suggests the Upper Dajia is evolving in similar ways to how it has in the past.

5.1.1 Terraces and Other Relict Features

Laterally Incising Meanders

As discussed in Chapter 2, simultaneous lateral and vertical incision will leave multiple flights of strath terraces within an individual meander bend (such as the modeled and field examples shown in Figure 6 and 16). This observation provides evidence that this incisional channel is also actively meandering. A prediction can be drawn that these are developed within the system mechanics over time rather than pulses driven by typhoons or earthquakes. This evolution may be the cause of the small knickpoints upstream of the evolving meanders as local base level changes as can be found in the locations of the blue triangles in Figure 16.

Abandoned Channels

A large abandoned meander in the study area, referred to as the Huanshan site, is ~75m above the modern channel and indicates that the Upper Dajia River has meandered in the past similarly to how it does today (Figure 17, RED box in Figure 9). The Huanshan site is characteristic of a river valley morphology, with steep valley walls, terraces, and a valley width similar to the modern Upper Dajia. Additionally, large rounded boulders can be found on the paleo-banks of this channel, which are indicative of erosional processes linked to past fluvial incision (Figures 18).

Figure 17b shows another abandoned channel in the lower region of the Upper Dajia that is yet to be explored in the field. This channel is ~130m above the modern channel and is the paleo-flood path of either the Dajia or the Sijilang tributary, further field confirmation is required to determine its potential origin.

5.1.2 Valley Width and Width Scaling:
Controls on channel width

Valley widths extracted from the *ChanGeom* algorithm indicate that widths in this area of Taiwan are very inconsistent, ranging from < 5m to ~300m in very short distances. This variation is due to a multitude of reasons, some autogenic (or internal within the drainage system) or allogenic (beyond the system). One of the most common disruptions in this region is due to landslide dams. Debris dumped into the channel constricts flow, limiting incision capability upstream of the dam and causing a decreased in slope as the channel begins to fill rather than incise. Immediately downstream of the dam, incision capability is increased due to the increased slope and constriction of channel. An example is shown in Figure 19.

5.2 LANYANG CAPTURE

As seen in Figure 13, measured width is greatly overestimated both by all scaling methods. Although the flooded-valley width is used to represent measured width, the difference from the scaled width is underestimated much more significantly. It can be hypothesized that this wide, “under-utilized” valley once supported much more drainage contribution than it currently is, shown by the large jump in width from the headwater channel that were once just a side-tributary (Figure 13, GREEN in Figure 22 (bottom)). Observations both in the field and through areal imagery support the hypothesis that the

large valley at the head of the Dajia is largely underfed, leading to the hypothesis that the Dajia watershed is losing drainage area to the Lanyang watershed (Figure 20, 21).

As discussed, drainage area has the most significant impact on incision capability. As drainage area is being lost, stream power in the Dajia River is reduced and lowers incision capability. This loss of capacity thus increases the amount of aggradation and leads to an overall reduction of the channel gradient (Figure 21). As discussed in Chapter 2, drainage basins in disequilibrium will undergo capture until equilibrium is met. As seen throughout this study, as well as in Figure 21, the Dajia has very low k_{sn} and unit stream power values while the Lanyang has very high k_{sn} values in its headwaters. Figure 22 shows a hypothetical model of the evolution occurring in this region as the two drainage basins fight for equilibrium. Other models of incision capability such as chi analysis (χ) also support the hypothesis that the Lanyang River is capturing the Dajia as well (Willett and Chen, 2014).

Observation of modern tectonics of the region may provide evidence as to why the Lanyang basin is able capture the Dajia. The Lanyang River drains northeastward to the Yilan Plain. As discussed in Chapter 2, the Yilan Plain is an extension of the Okinawa trough and is actively spreading (e.g. Figure 2; Ching et al., 2000; Lin et al., 2010). This increase in drainage area, increase in subsidence, as well as uplift in the Central Range allow for an increase in incision capability in the Lanyang drainage basin. The increase in dilatation as well as clockwise rotation of GPS stations spreading (Lin et al., 2010) alongside the downward movement along the Yilan plain indicated in highway leveling data (Ching et al., 2000) can further support this hypothesis.

CHAPTER SIX: CONCLUSIONS AND FUTURE RESEARCH

6.1 CONCLUSIONS

Bedrock channel incision plays an important role on the overall evolution of mountainous topography (e.g. Seidl and Dietrich, 1992; Burbank et al., 1996; Finnegan et al., 2005). Previous studies have found that steep, alluviated bedrock channels can actively evolve both vertically and laterally and leave traces on the landscape in the form of terraces and relict features. These features indicate active evolution within meanders and knickpoints in channels (e.g. Finnegan and Dietrich, 2011; Finnegan et al., 2004; Finnegan and Balco, 2013; Hartshorn et al., 2002; Turowski et al., 2007). This evolution results from allogenic impacts like climate change or tectonically induced changes in incision or deposition, or autogenic impacts such as localized landslide dams and laterally incising meanders (e.g. Dadson et al., 2003; Liew and Hsieh, 2001; Hsieh and Capart, 2013; Kirby and Ouimet, 2011;.Stark et al., 2010).

A channel's ability to incise depends on variables with in the geomorphology of the region including discharge (which is approximated by contributing drainage area in this study), width, and longitudinal slope. A channel in a highly tectonically and climatically active region, such as the upper Dajia, often experiences disruption in these indices that further disrupt a channel's ability to incise. Through the usage of k_{sn} and unit stream power, incision capability can be estimated and further used to understand the past and present evolution of a channel.

6.2 FUTURE RESEARCH

To further understand the geomorphic evolution of this drainage basin and in Taiwan, especially tectonic and climate history, dates for the terraces and abandoned features in this region are crucial. With dates, rates of evolution, such as incision and

uplift can be calculated and modeled and their controls can be further investigated. Recent studies have found evidence of climate fluctuations that have likely triggered periods of mass erosion and aggradation, including the Lanyang River, during the late Holocene (Liew and Hsieh, 2000; Hsieh and Knuepfer, 2001; Hsieh and Capart, 2013). Dates from terraces in both the Lanyang and Dajia watersheds can be used to further understand the hypothesized capture by modeling previous channel geometries back through time. More comprehensive field mapping will also be performed to further classify terraces/ abandoned features and landslide dams.

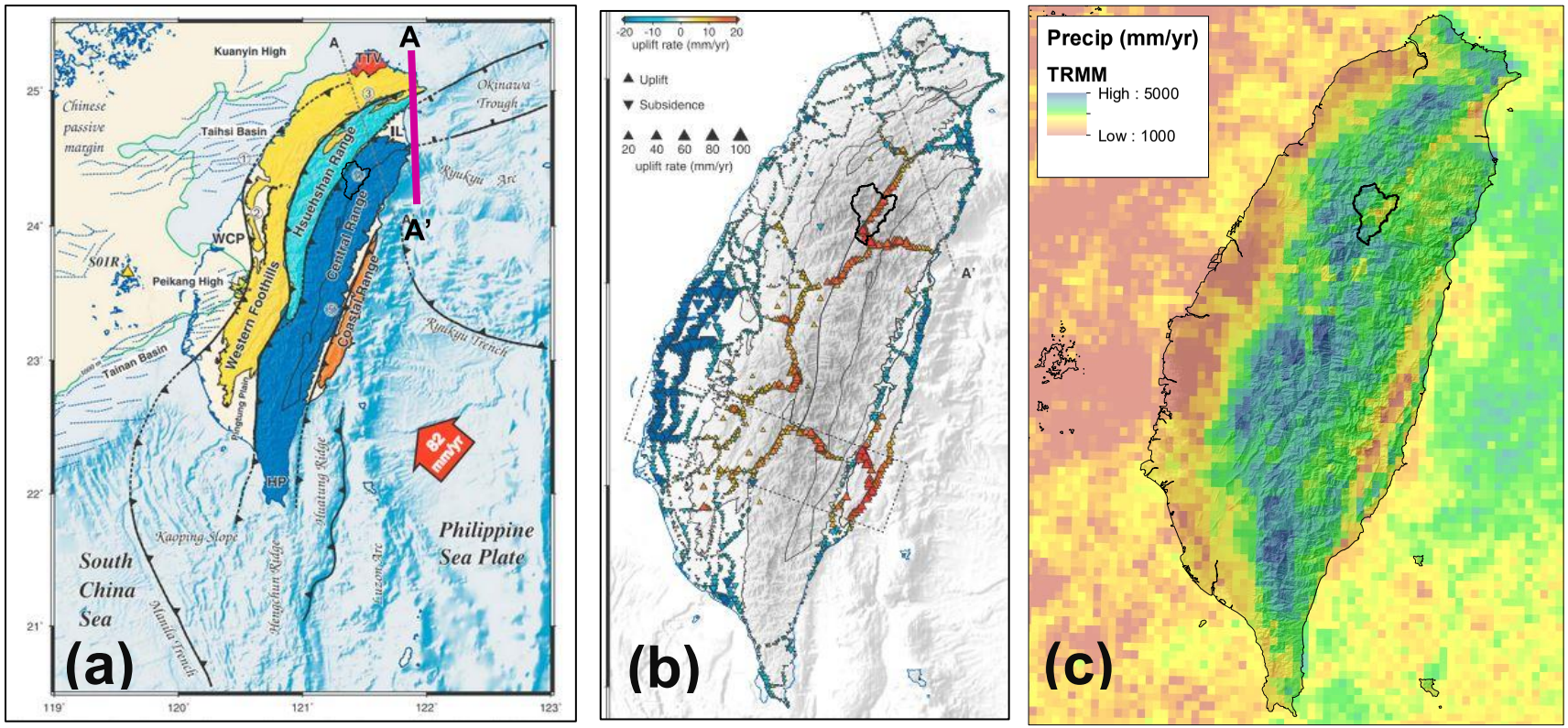

Figure 1. Tectonic and climate summary for the island of Taiwan. (a) General geologic/ tectonic map (Ching et al., 2000) cross section shown in Figure 2d., (b) Tectonic uplift and subsidence based off of GPS and highway leveling data (Ching et al., 2000), (c) TRMM precipitation data (Bookhagen).

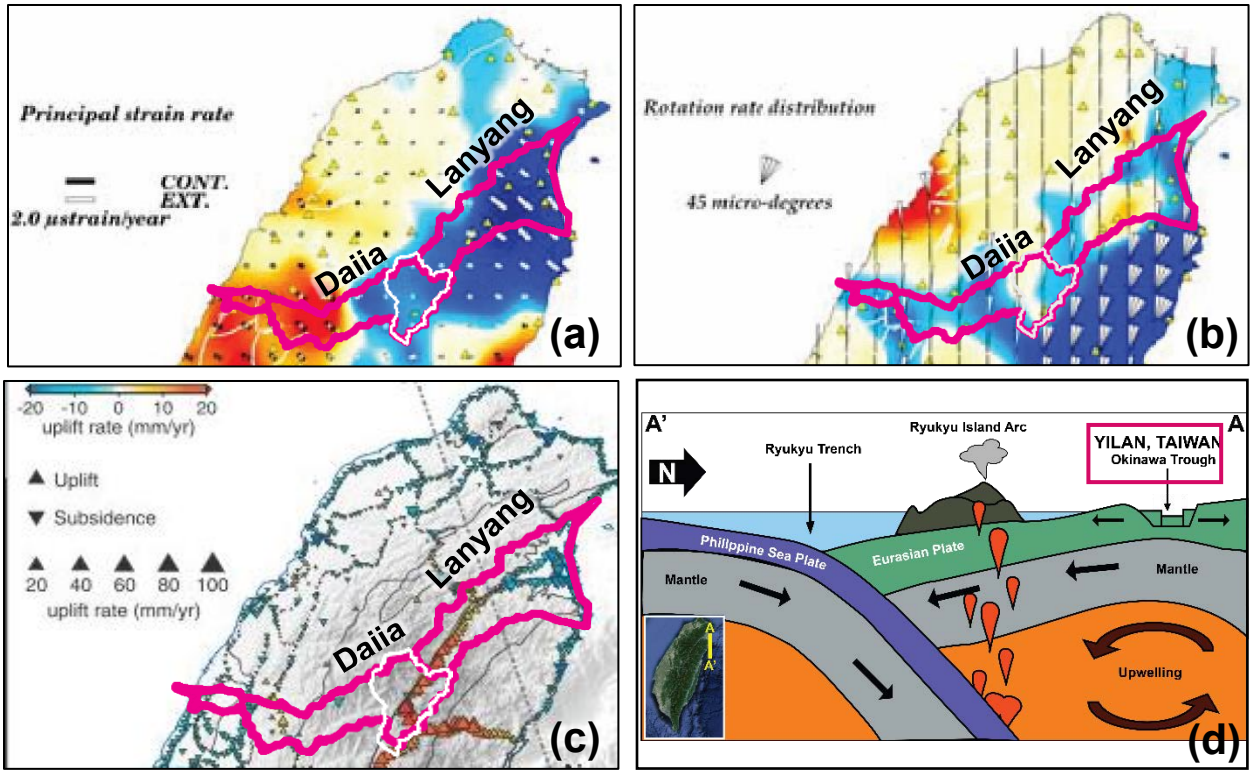

Figure 2: Northern Taiwan summary. (a-c) GPS and highway leveling data (Ching et al., 2000 and Lin et al., 2010. (a) Strain/horizontal movement data; (b) Rotational data; (c) Vertical movement data. (d) Model of tectonic drivers that causes the spreading of the Yilan Plain – the mouth of the Lanyang River. Pink indicates drainage basins discussed in Section 5.3.

Figure 3. Examples of alluvial-bedrock rivers in Taiwan. (a) Intense alluvial aggradation followed by subsequent incision of <10m (Ailiao River – S. Taiwan); (b) Taroko Gorge; (c) Tienhsiang.

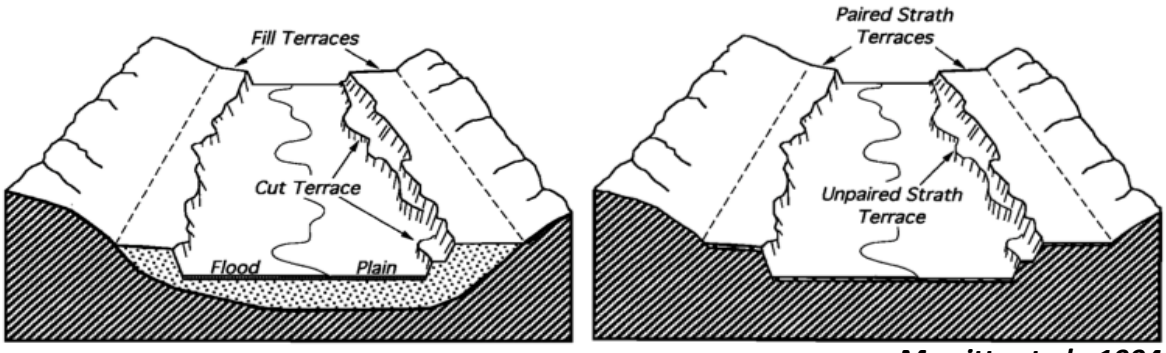

Merritts et al., 1994

Fill Terraces

- **Abandoned alluvial surface**
- **Formed in alluvial sediments (sand and gravel) now well above the normal level of inundation**
- **Reflect fluvial/alluvial aggradation, then incision**
- **Fill, cut-fill types…**

Strath Terraces

- **Erosional terrace cut into bedrock (may have a capping of alluvial sediments)**
- **Reflect incision of river into bedrock**

Figure 4. Comparison of fill and strath terraces. Fill and strath terraces may look similar in plan view until their materials are observed.

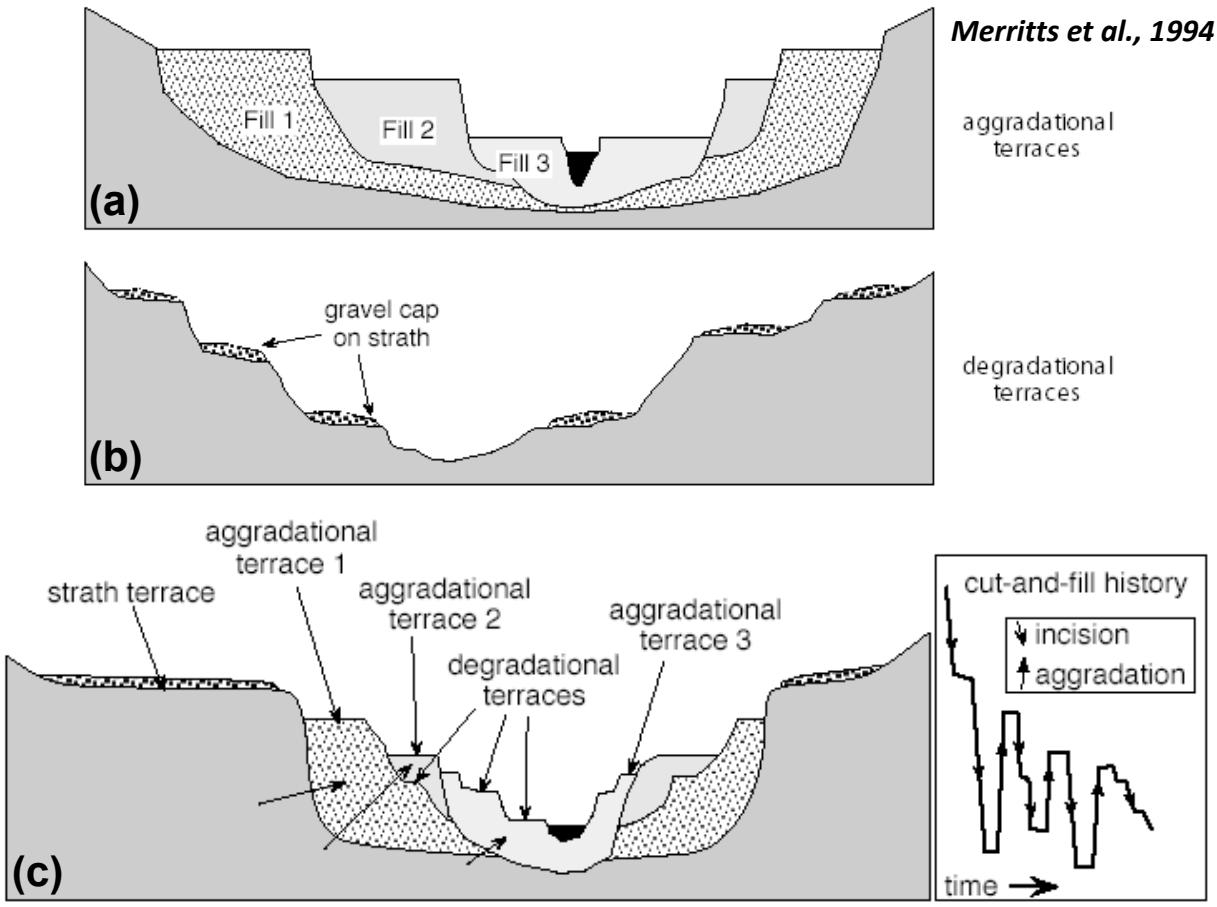

Figure 5. Terraces form due to changes in sediment supply (Q_s), changes in water discharge (Q_w), and adjustment to base level rise/fall. (a) Fill and cut sequences are aggradational, usually are related to climatic cycles. (b) Strath terraces are degradational and form from continuous downcutting due to tectonics (uplift, base-level fall). (c) Higher strath levels related to long-term incision with inset climate related fill terraces is common.

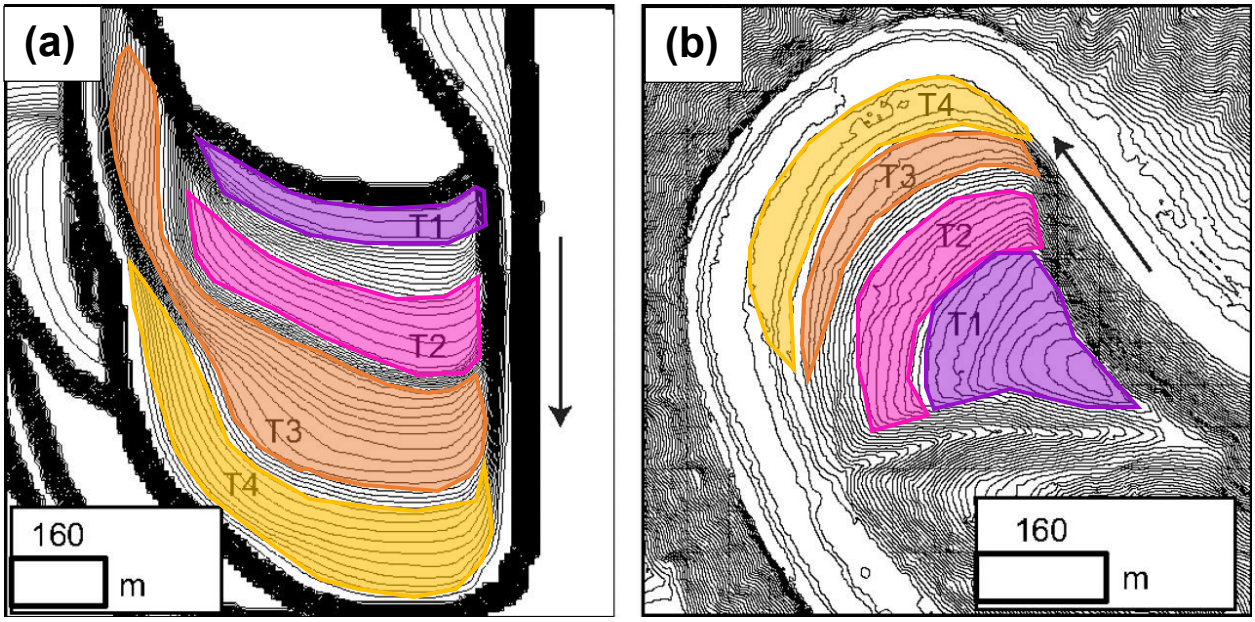

Figure 6. Meander evolution and strath terrace formation modified from Finnegan and Dietrich, 2011; Strath terraces are labeled as T1–T4 (oldest to youngest). Contour interval is 3 m in all images. Black arrows in (a) and (b) indicate river flow direction. Contour maps of stepped meander bend. (a) Result from numerical simulation. (b) Smith River, Oregon LIDAR data.

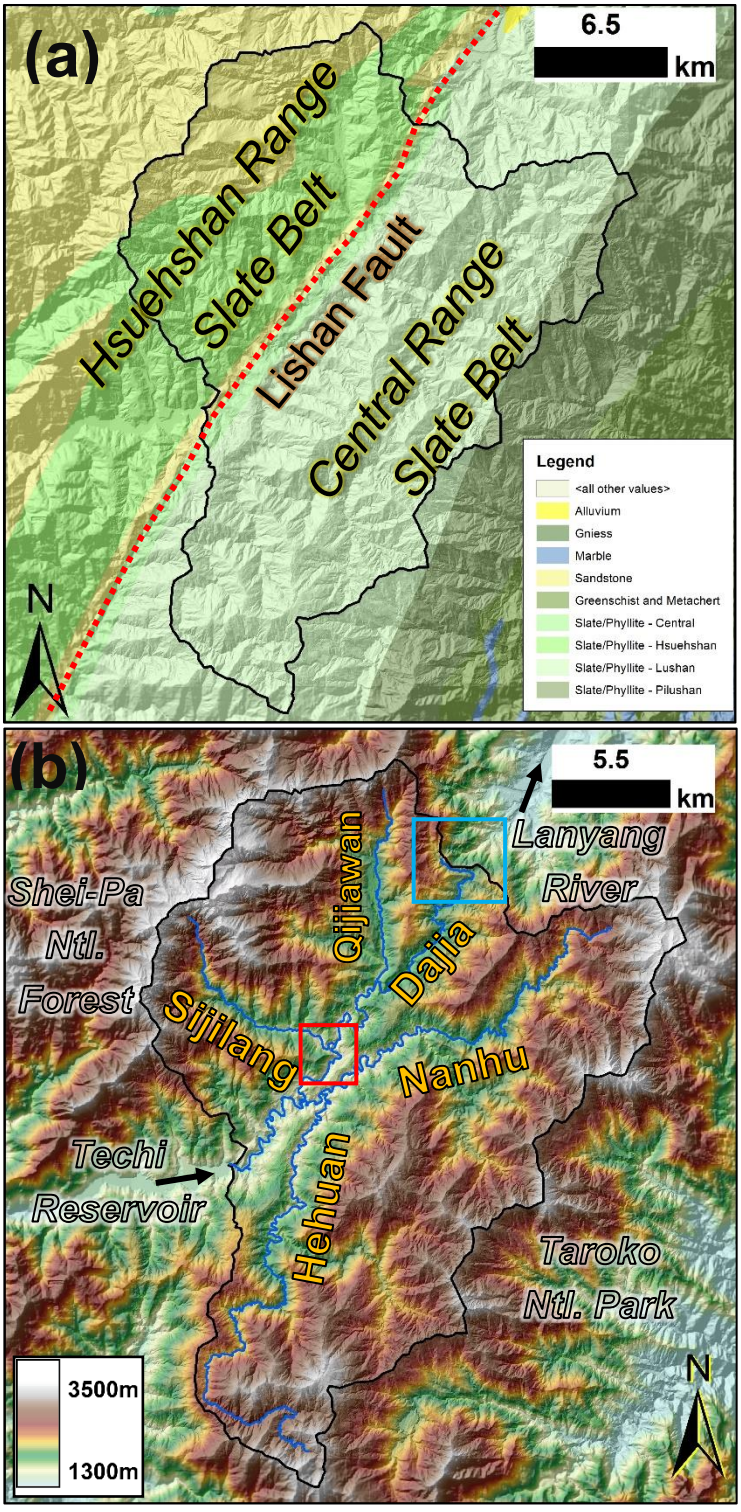

Figure 7. Upper Dajia drainage basin. (a) Geology of the study area, (b) DEM of the study area, with surrounding areas of interest (white labels) and studied channels (gold labels); RED BOX indicates region of discussion in Figures 17,18; BLUE BOX indicates region of river capture discussion (Figures 20-22)

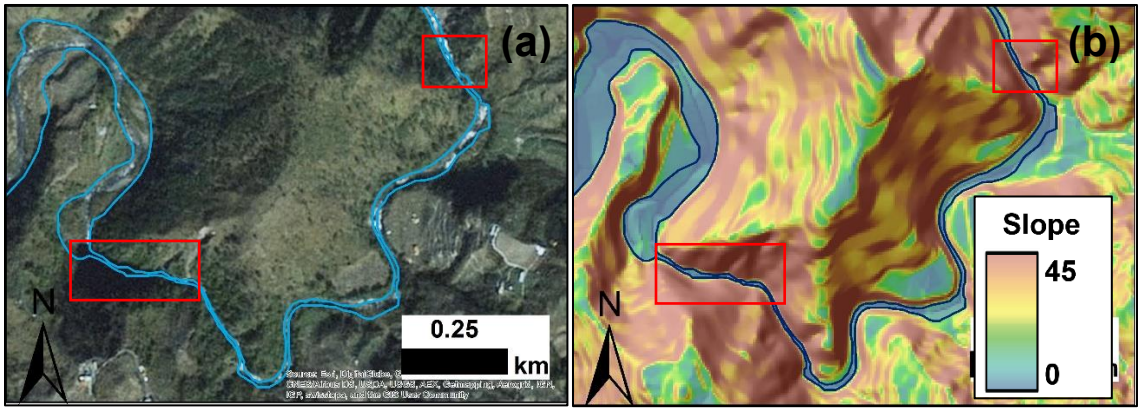

Figure 8. (a) Areal imagery from Google Earth, (b) 5m DEM slope map. Slope map used to map valley widths to eliminate potential errors from grainy imagery and dense vegetation - boxes indicate examples that would be difficult to trace accurately.

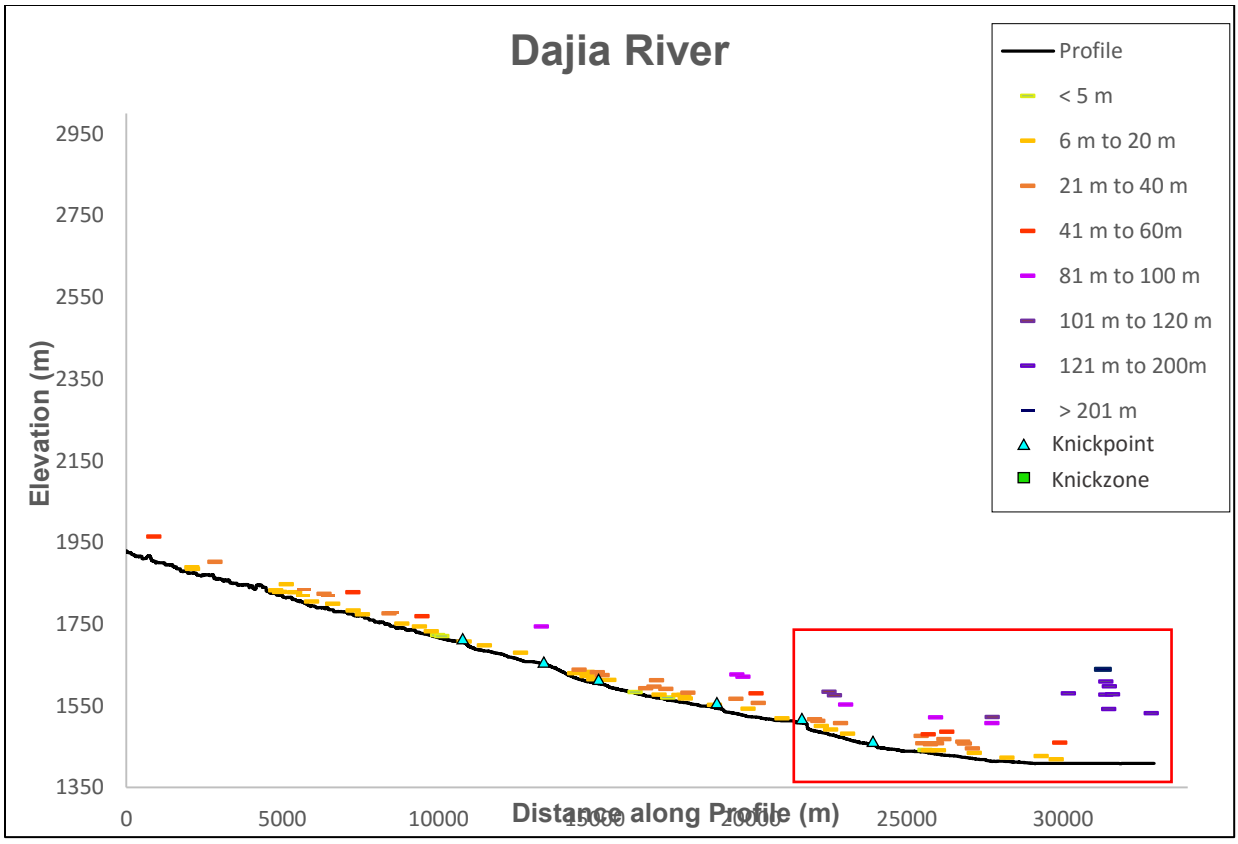
Dajia River
Profile
< 5 m
6 m to 20 m
21 m to 40 m
41 m to 60m
81 m to 100 m
101 m to 120 m
121 m to 200m
> 201 m
Knickpoint
Knickzone
Elevation (m)
2950
2750
2550
2350
2150
1950
1750
1550
1350
0
5000
10000
15000
20000
25000
30000
Distance along Profile (m)

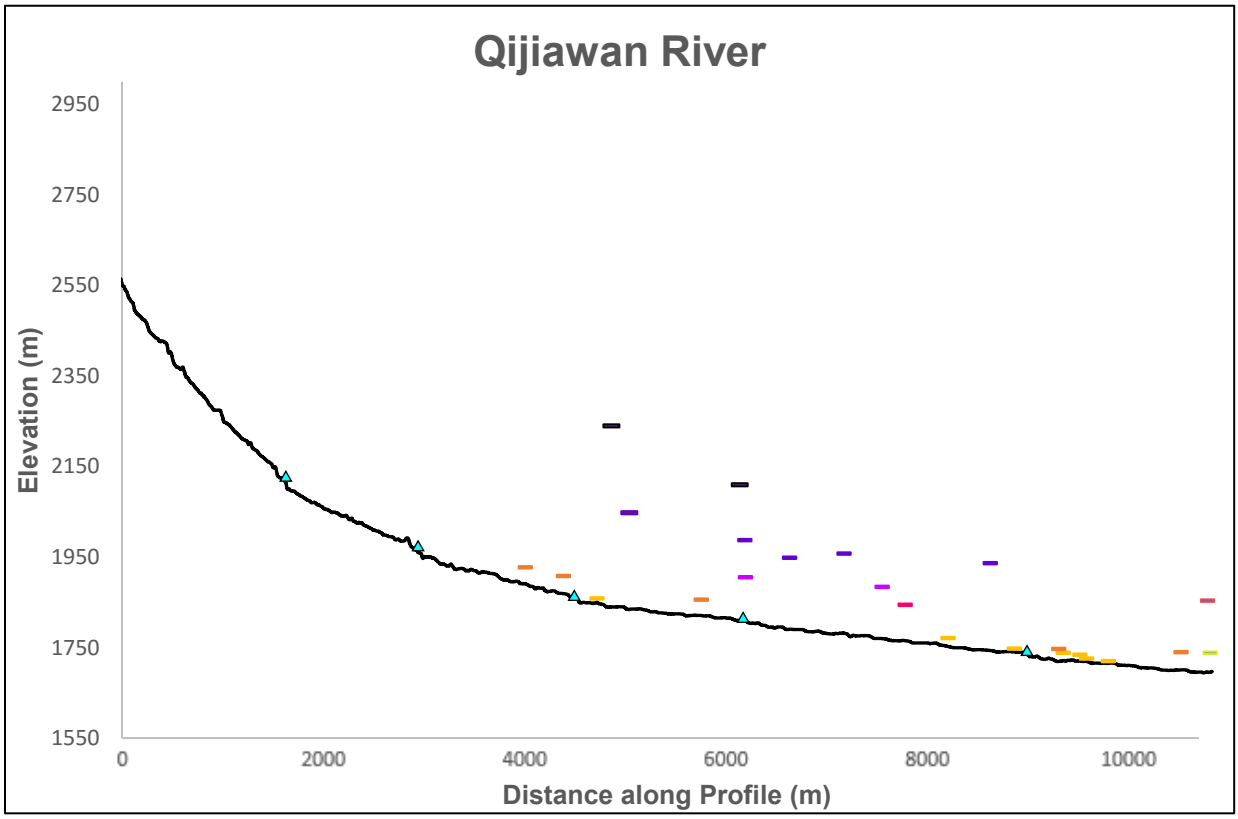
Qijiawan River
Elevation (m)
2950
2750
2550
2350
2150
1950
1750
1550
0
2000
4000
6000
8000
10000
Distance along Profile (m)

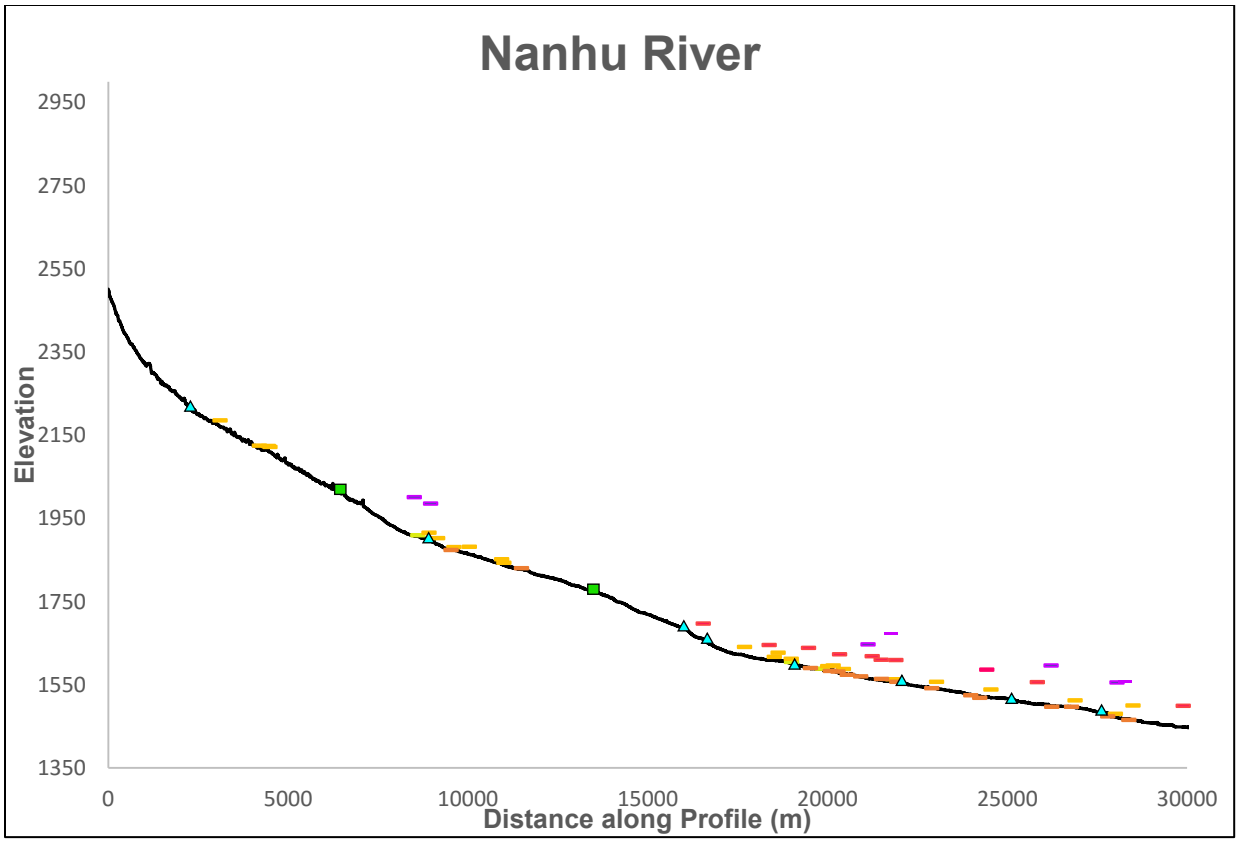
Nanhu River
Elevation
2950
2750
2550
2350
2150
1950
1750
1550
1350
0
5000
10000
15000
20000
25000
30000
Distance along Profile (m)

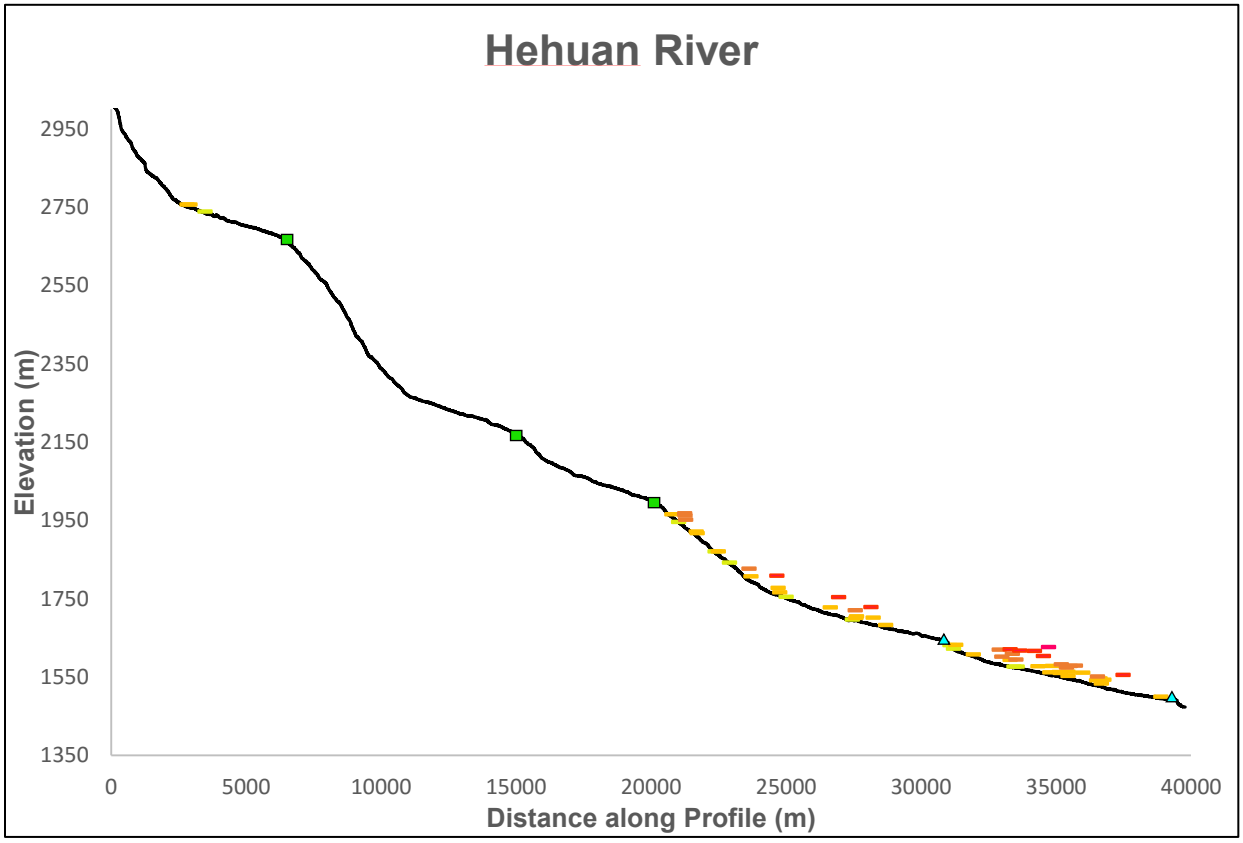
Hehuan River
Elevation (m)
2950
2750
2550
2350
2150
1950
1750
1550
1350
0
5000
10000
15000
20000
25000
30000
35000
40000
Distance along Profile (m)

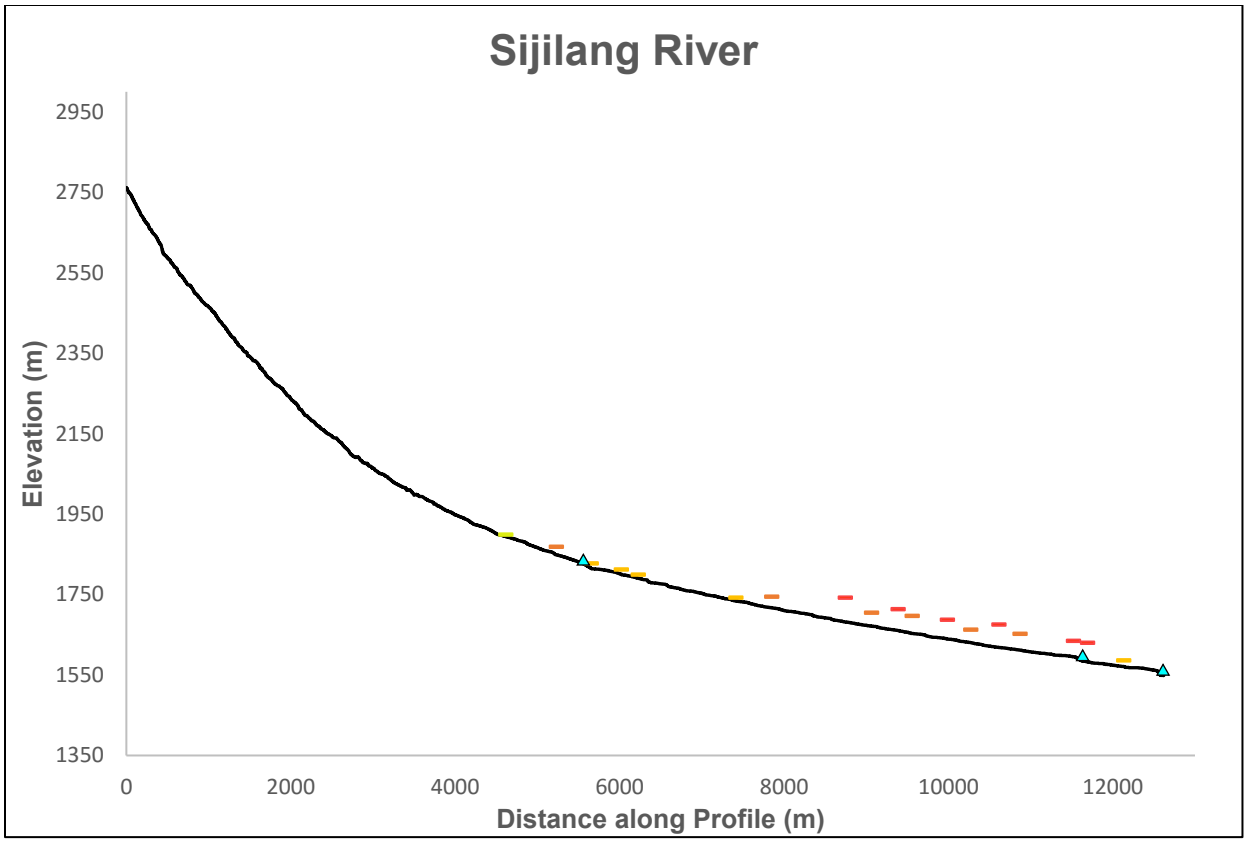

Figure 9. Longitudinal profiles and adjacent mapped river terraces for the Dajia, Qijiawan, Nanhu, Hehuan, and Sijilang Rivers. Colors to show preliminary height correlations. RED BOX indicates area in Figures 13, 14.

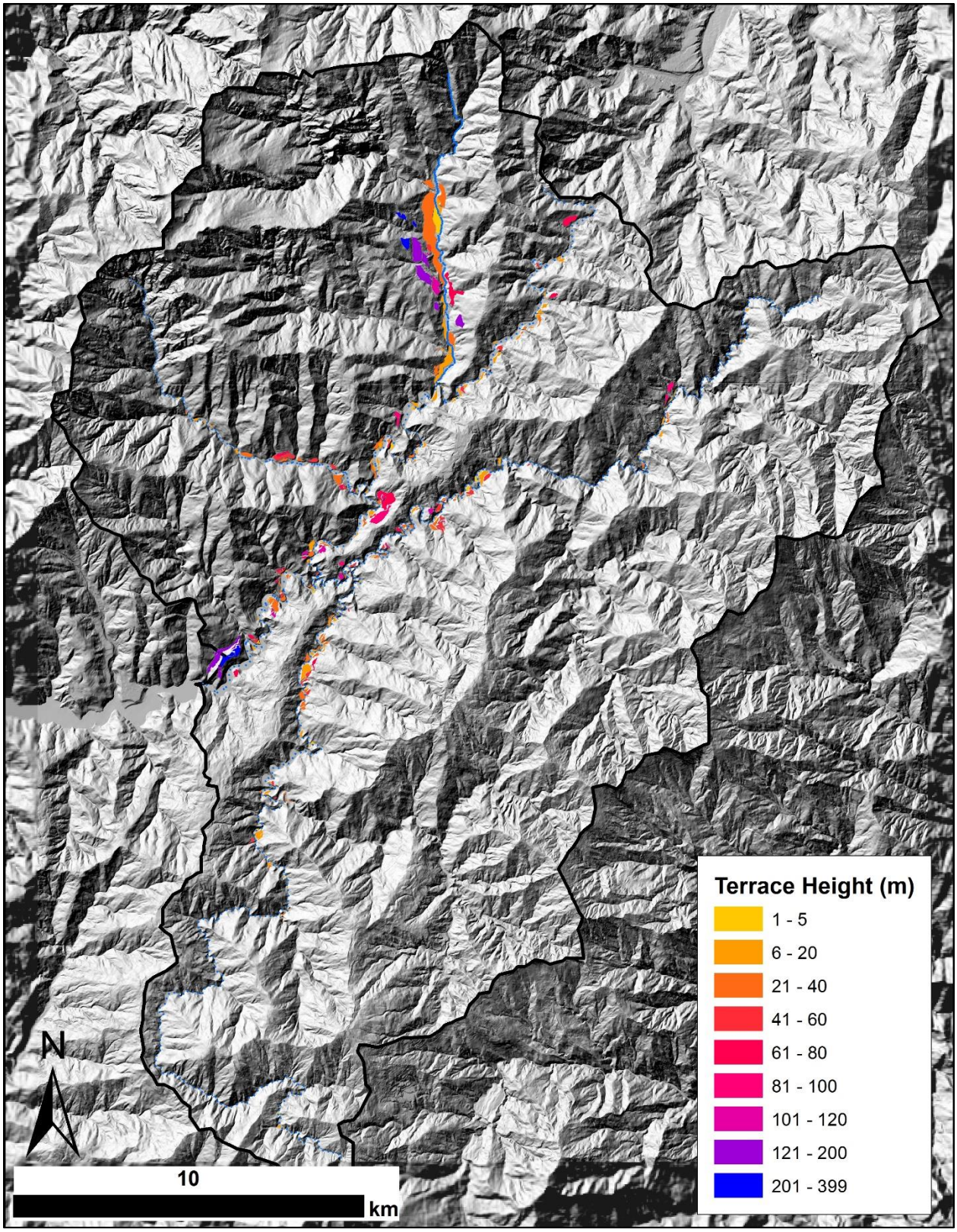

Figure 10. Terrace map of the Upper Dajia. Preliminary correlations are shown by height.

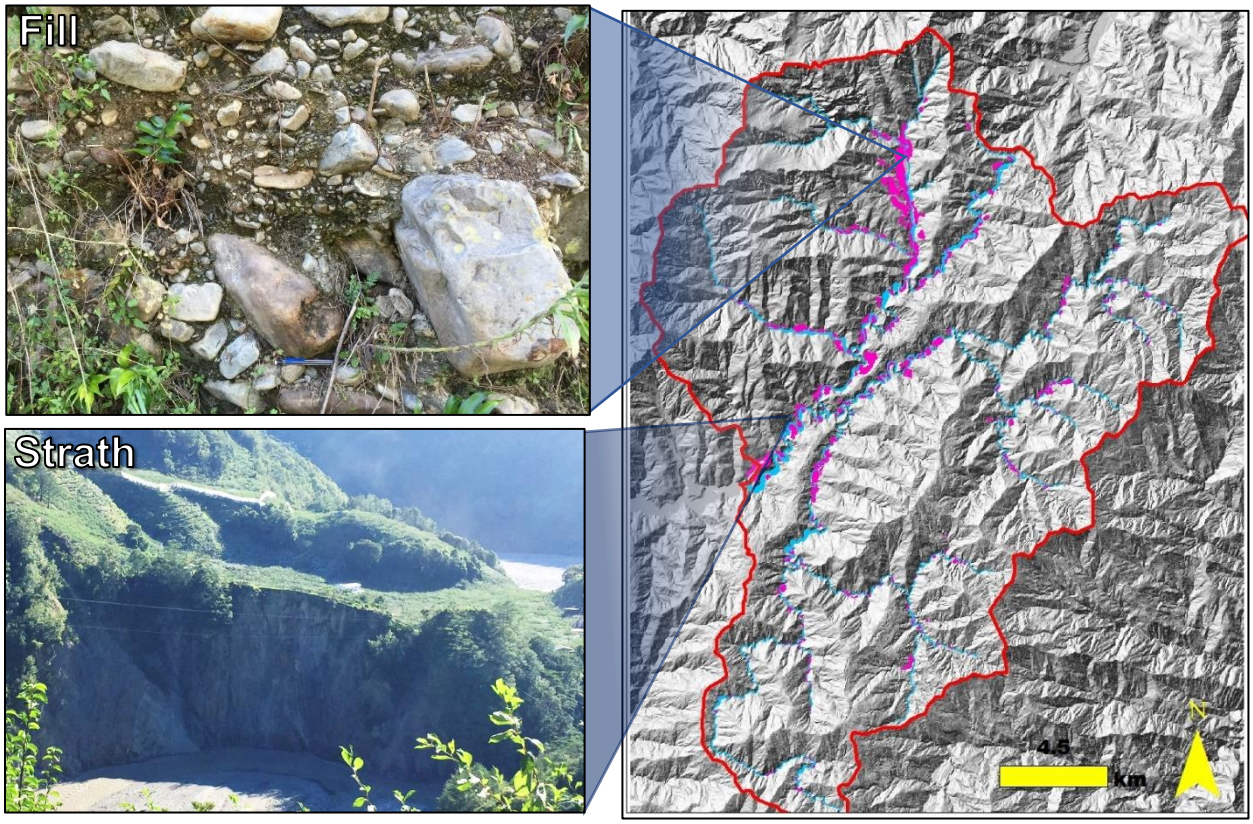

Figure 11. Examples of types of terraces in the study – Fill terraces composed of sediment ranging from fine grained to rounded boulders; Strath terraces composed of bedrock.

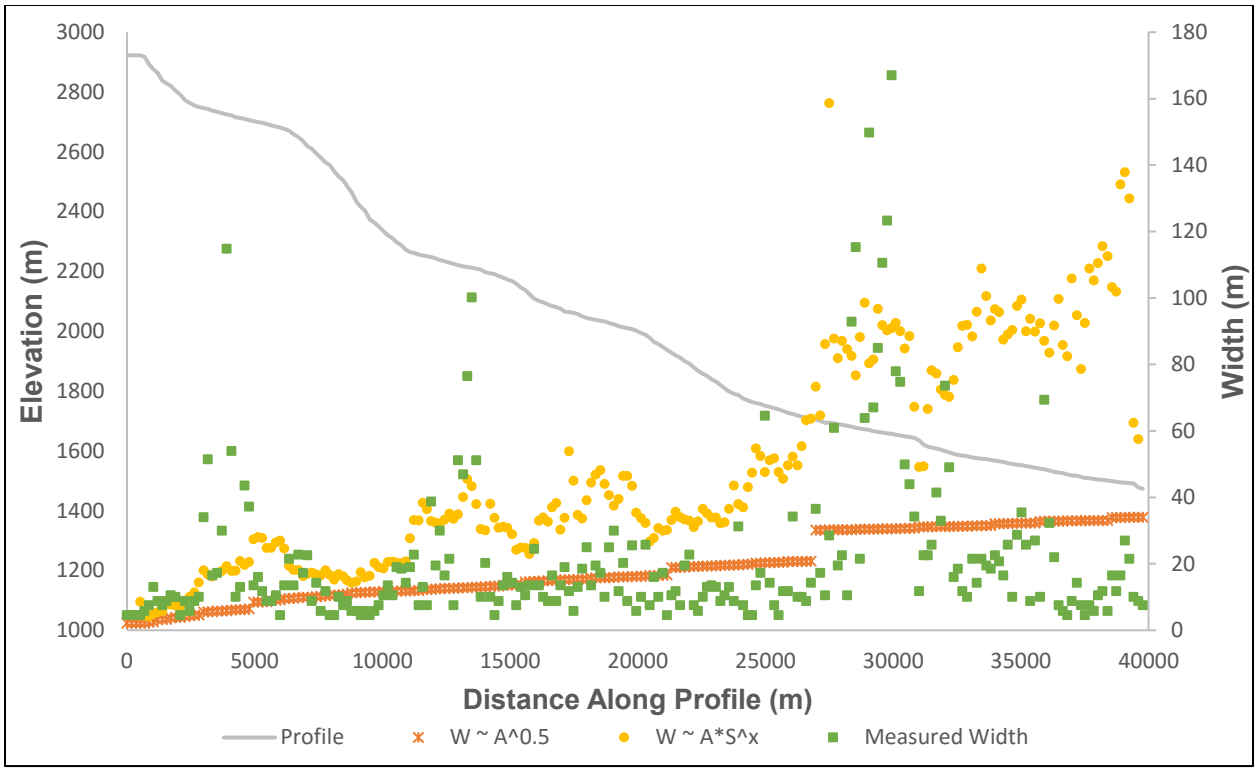

Figure 12. Hehuan Valley Width and Longitudinal Profile. Flooded valley width comparisons with longitudinal profile.

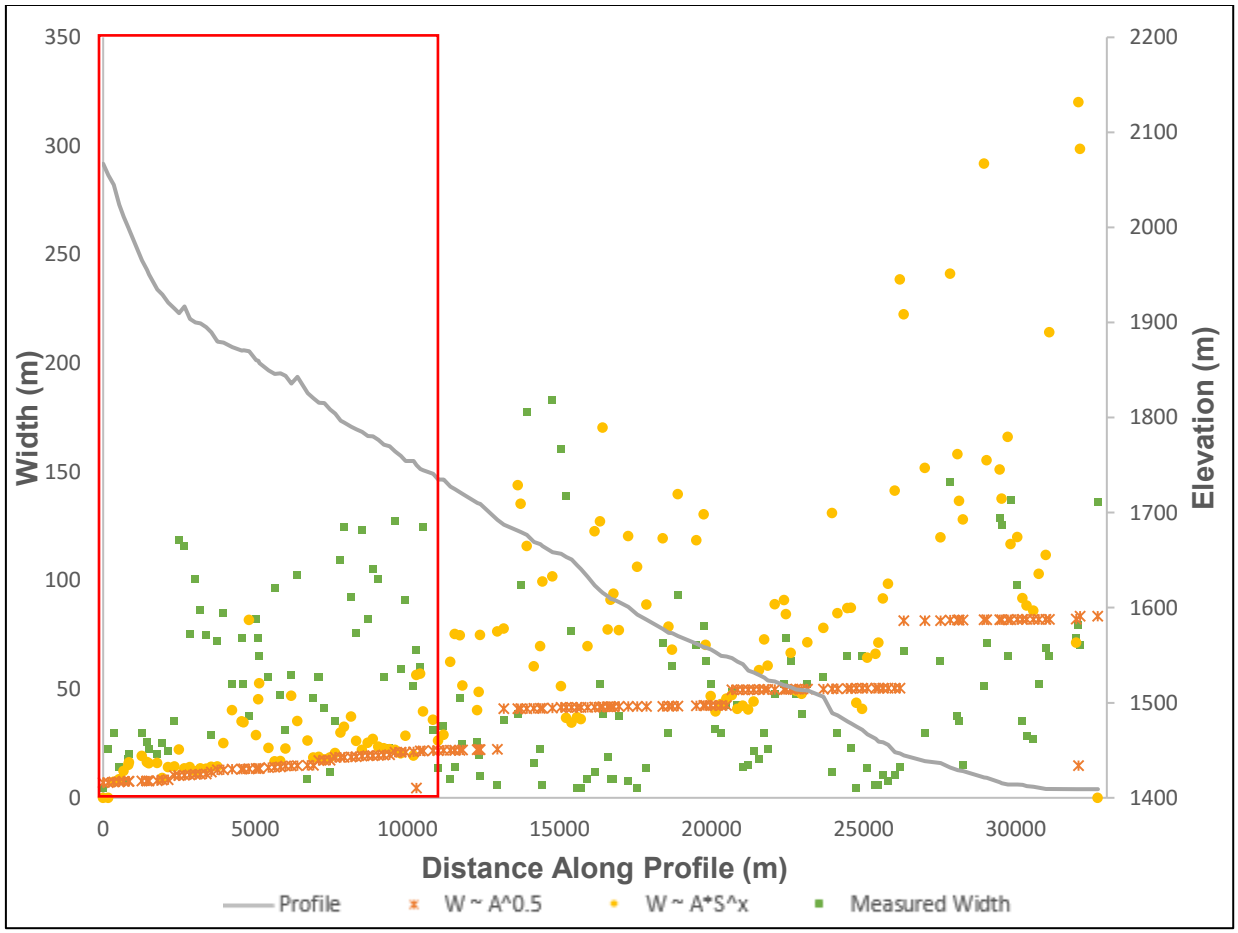

Figure 13. Dajia Valley Width and Longitudinal Profile. Flooded valley width comparisons with longitudinal profile. Red box refers to discussion in Section 5.3.

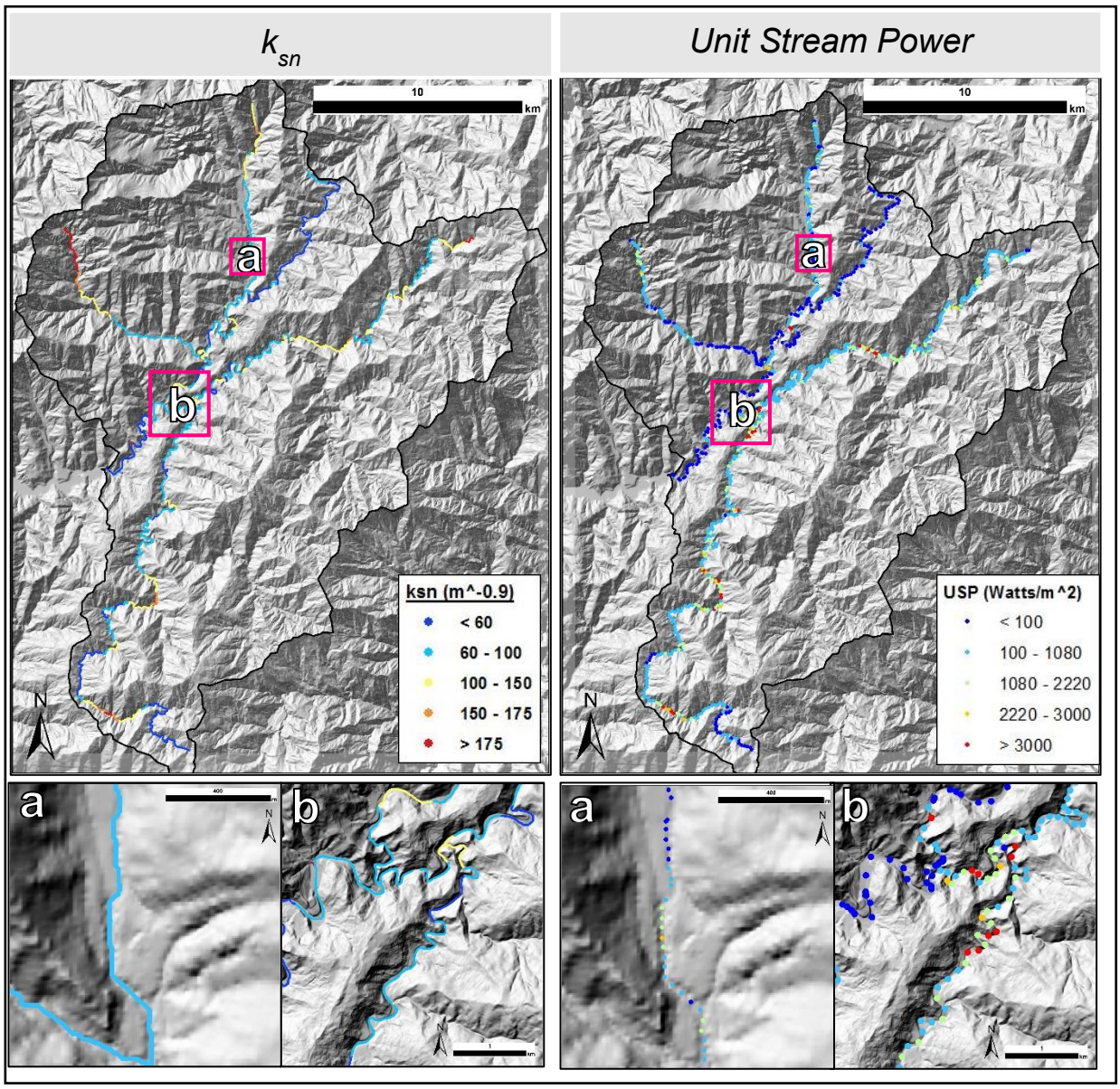

Figure 14. ksn (left and unit stream power (right) plots of the studied channels. Examples of how the two methods of quantifying incision capability differ – (a) Qijiawan landslide dam, (b) Confluence of Hehuan and Nanhu Rivers with the Dajia.

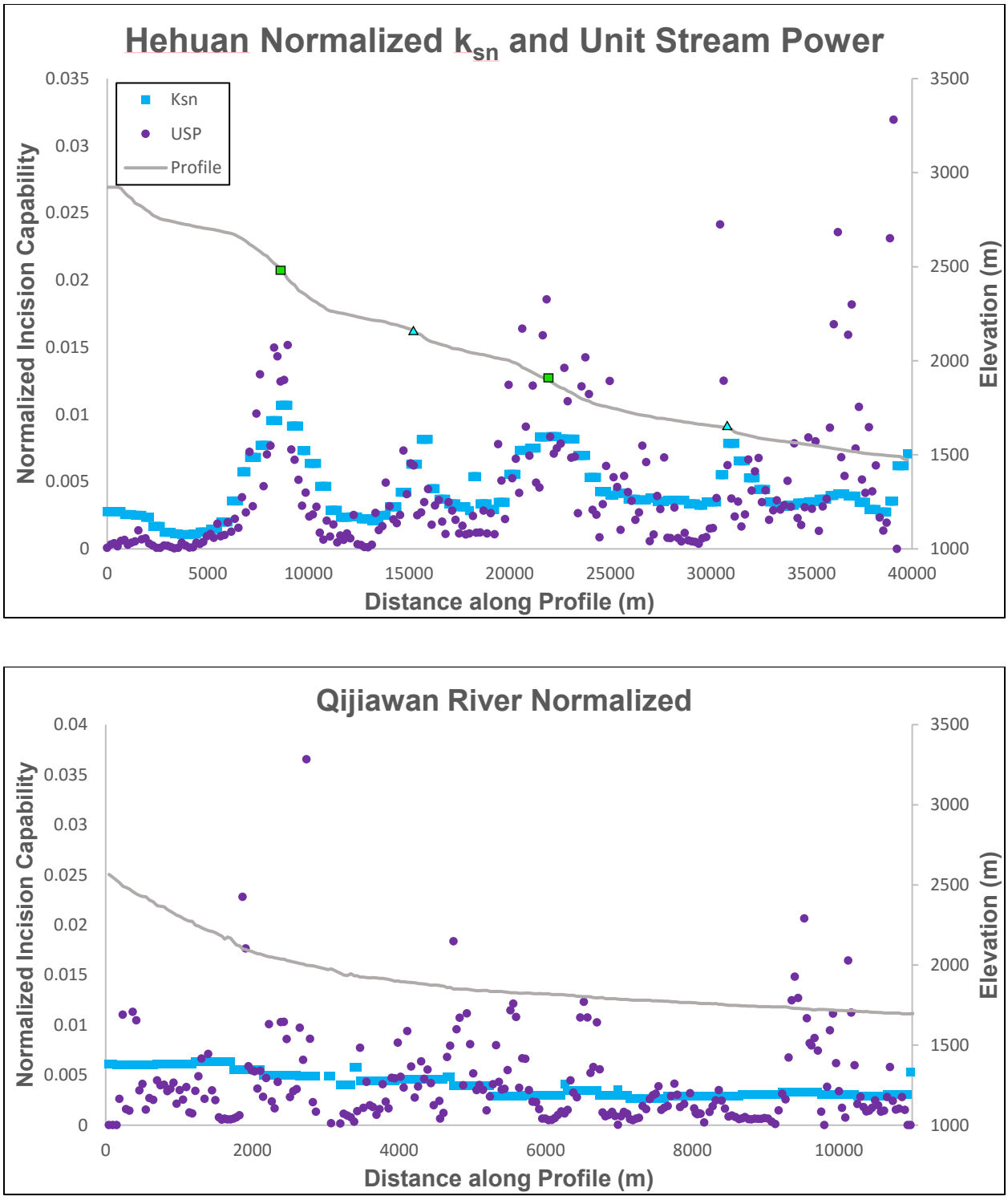

Figure 15. Comparison of k_{sn} (blue) and unit stream power (yellow) over longitudinal profile over the Hehuan River. Incision Capability methods were normalized to a value of 1.

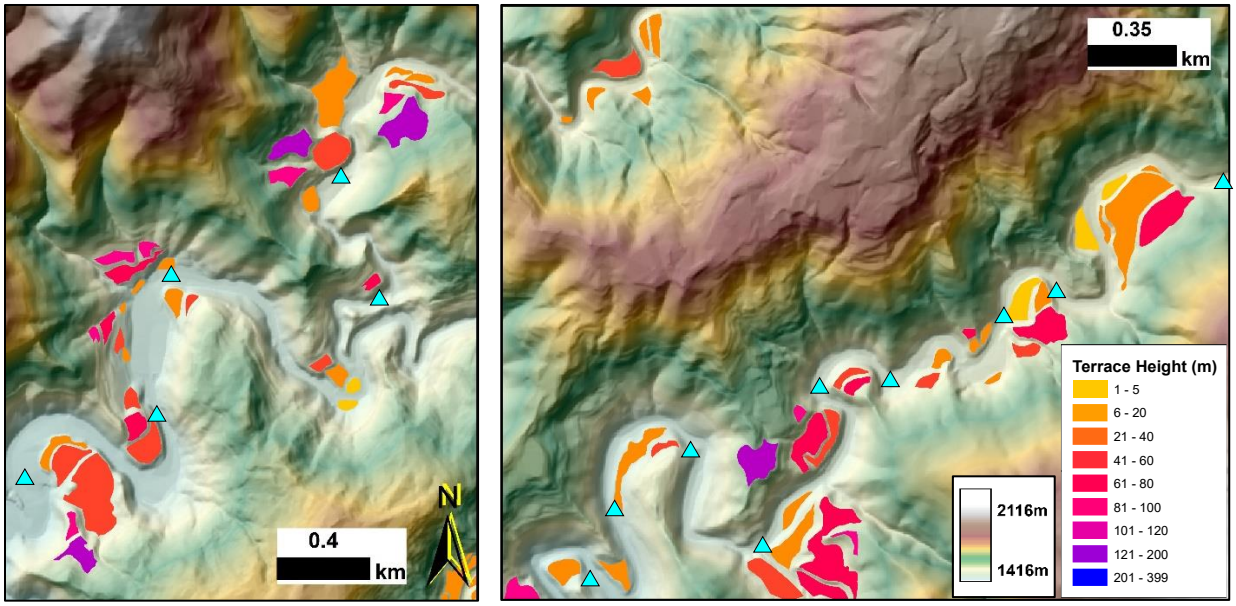

Figure 16. Examples of meander-bend terraces (follow the same color scheme as Figure 6). (Left) Dajia River at the confluence with the Nanhu. (Right) Nanhu River, lower channel; Dajia River, upper channel. Blue triangles represent small knickpoints.

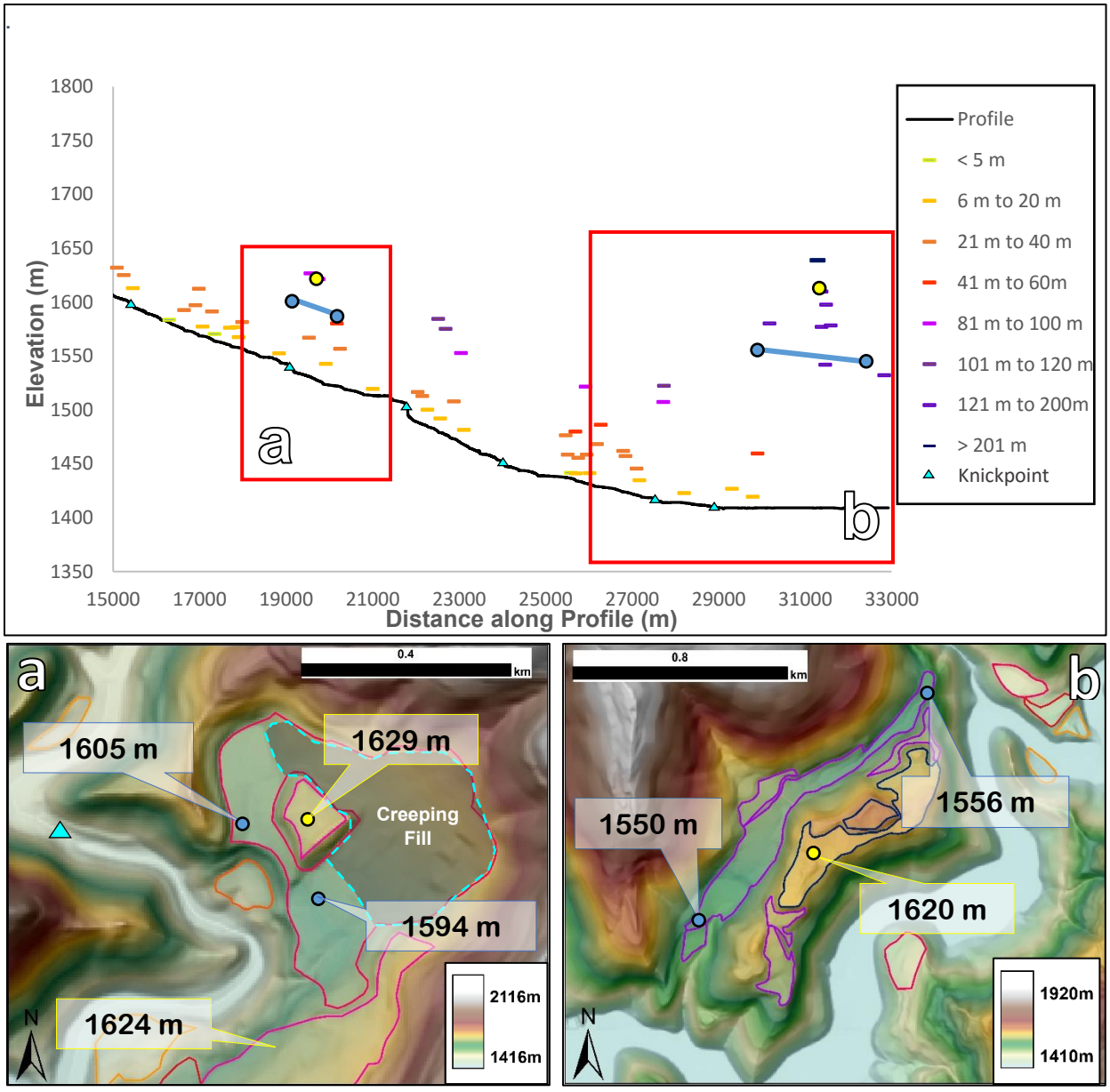

Figure 17. Relict channels along the Upper Dajia trunk river that occur within the RED BOX in Figure 9a. Blue lines show hypothesized pale-channels. Terrace colors in maps match profile. (a) Abandoned meander loop cutoff ~75m above modern channel that has partially been filled by creeping debris; (b) abandoned channel parallel too and ~130m above the modern channel.

Figure 18. (Top-Left) Photo taken from the 1629m marker in Figure 16a looking east. (Top right) Photo showing large rounded boulders at the photo location that are even older than the meander itself (camera lens cap with yellow arrow for scale). (Bottom) Paleo-entrance to the meander loop; dashed blue line shows paleo-cross-section, (star shows photo location (b)). Black arrows in index map show direction of photo.

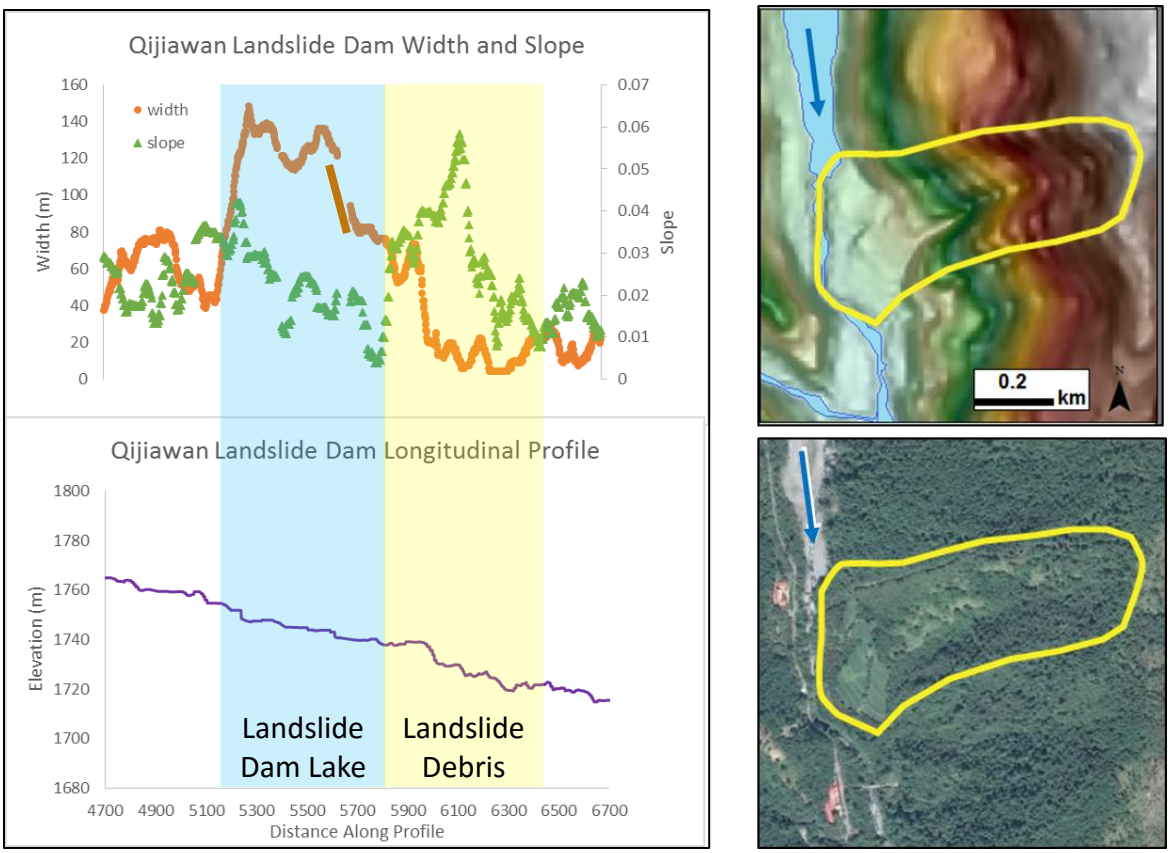

Figure 19. Example of how landslide dams impact a channel near the base of the Qijiawan Tributary – increase of width and decrease of slope before the knickpoints; decrease in slope and increase and slope after the knickpoint.

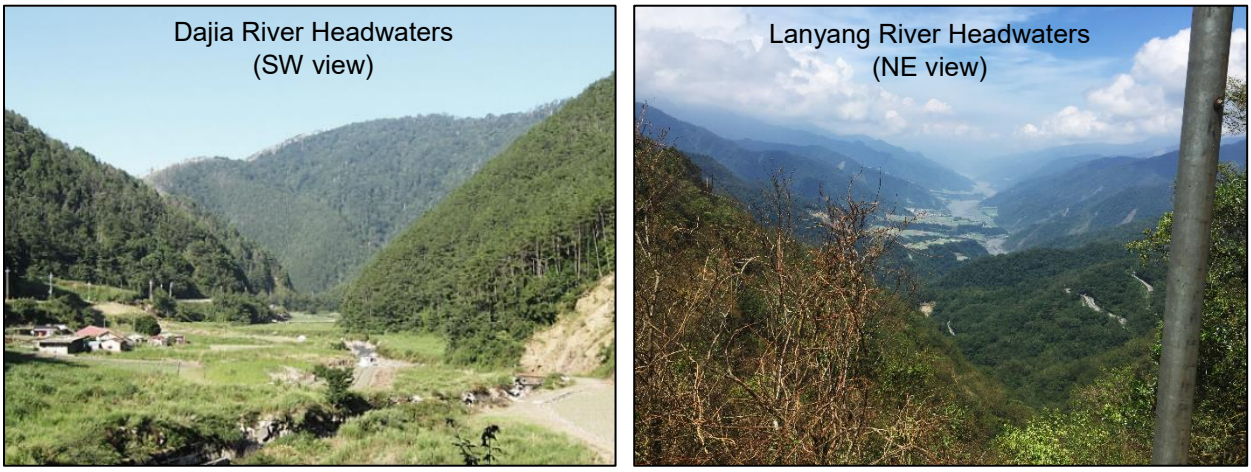

Figure 20. Downstream views from the headwaters of the Dajia and Lanyang Rivers. Note the difference in topography in the foreground; Dajia headwaters preserves a low relief valley floor whereas Lanyang preserves steeper slopes and higher relief. Dajia headwaters are interpreted to reflect reduction of drainage area by capture by the Lanyang River, resulting in a wind gap between the two drainages

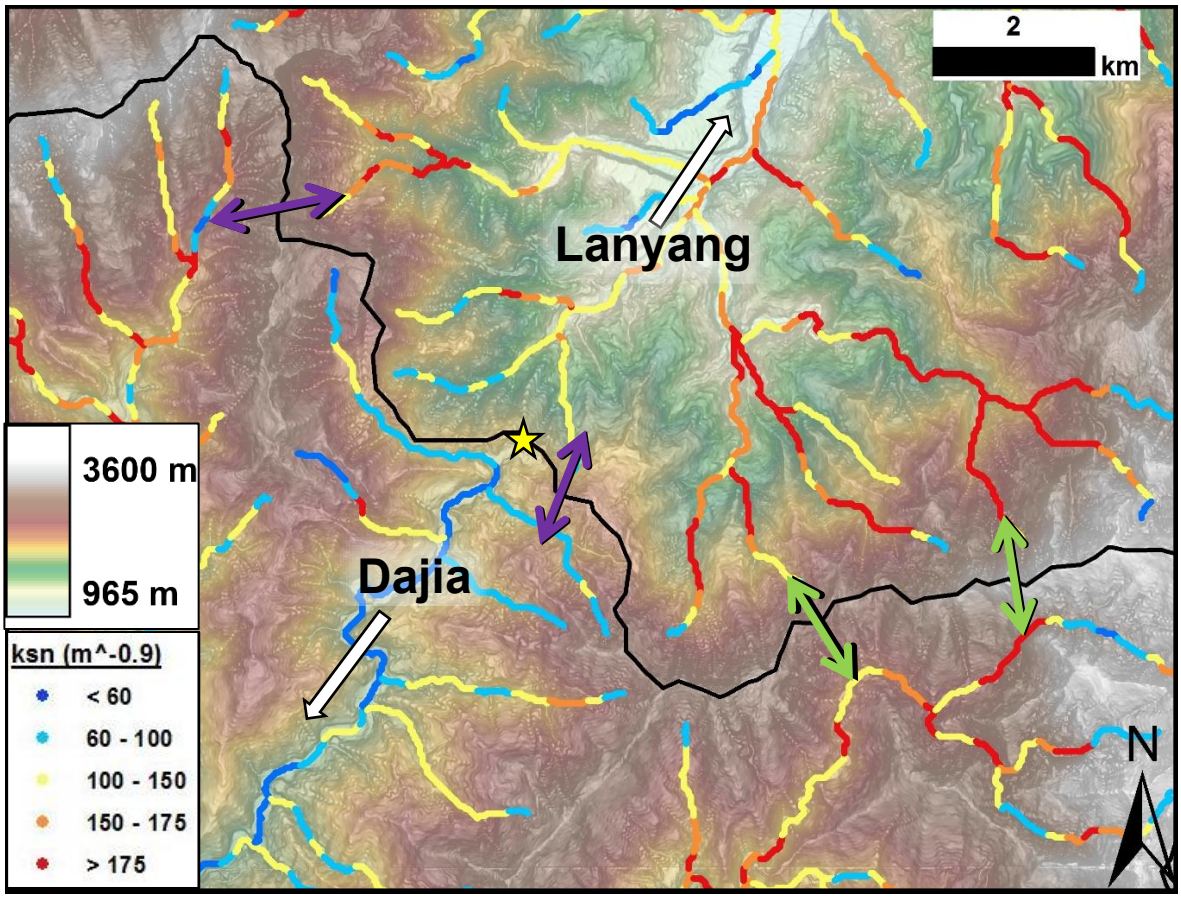

Figure 21. Higher k_{sn} values (red/warm colors) will incise into those that are lower (blue/cool). The Lanyang has more reaches with high k_{sn} values than the Dajia. WHITE arrows indicate flow direction, GREEN represents good cross ridge k_{sn} agreement where PURPLE represents poor agreement. (The pictured region is the BLUE BOX in Figure 7b). Star shows photo location for Figure 20.

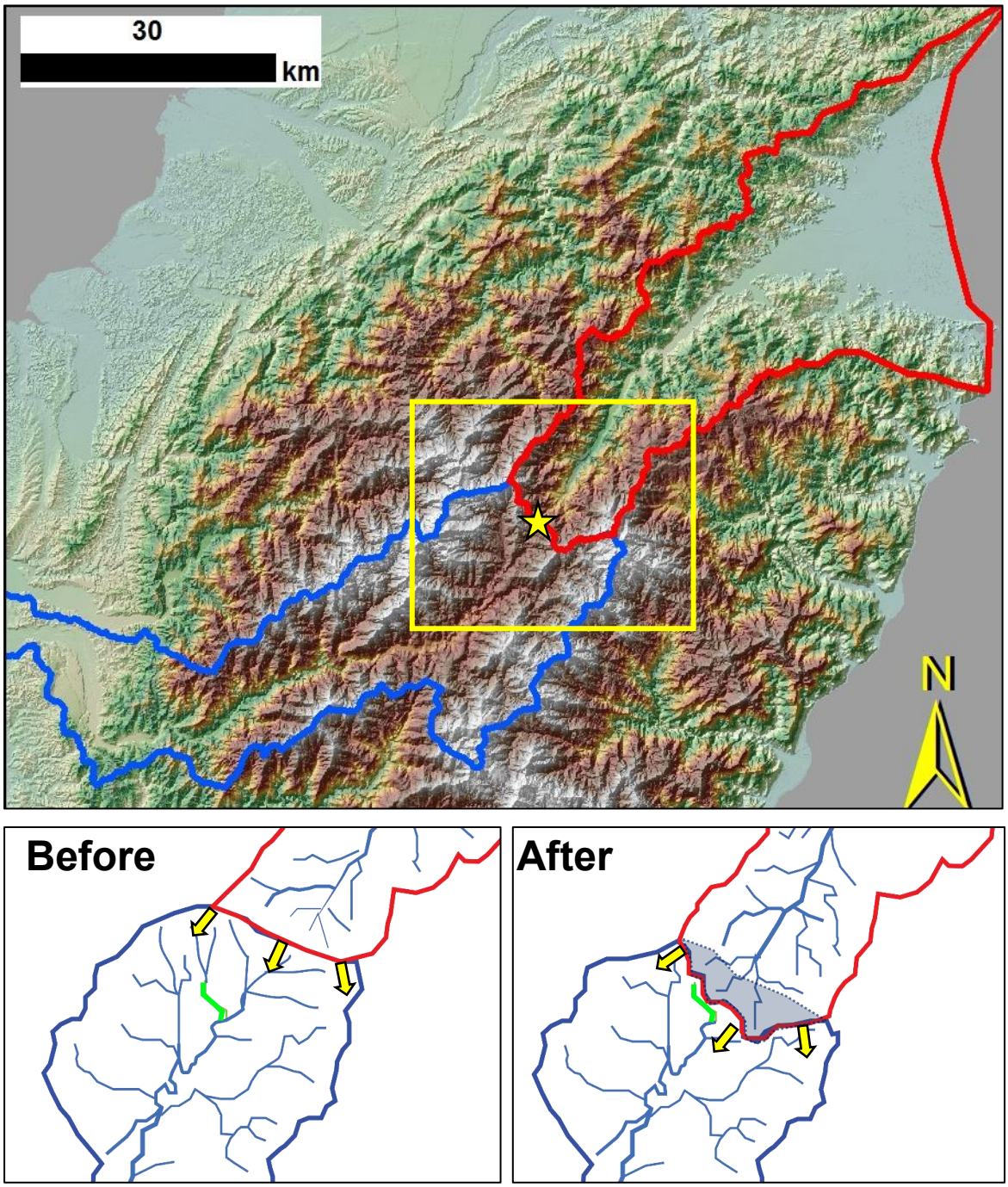

Figure 22. Hypothetical model of the Lanyang capture of the Dajia drainage basin. The green tributary in the bottom figures shows what was once a side tributary is now the head waters of the Dajia.

REFERENCES

Anderson, R.S., and Anderson, S.P., 2010, Geomorphology: The Mechanics and Chemistry of Landscapes, Cambridge University Press, 651 p.

Bookhagen, B., 2014. High resolution spatiotemporal distribution of rainfall seasonality and extreme events based on a 12-year TRMM time series.

Byrne, T., Chan, Y.-., Rau, R.-., Lu, C.-., Lee, Y.-., and Wang, Y.-., 2011, Chapter 8: The Arc–Continent Collision in Taiwan. *in Arc-Continent Collision*: Berlin, Heidelberg, Springer, p.213-245.

Central Geological Survey, M., 2016, Geology of Taiwan: <http://www.moeacgs.gov.tw/english/twgeol/twgeol_introduction.jsp> (01/14 2016).

Ching, K.-., Hsieh, M.-., Johnson, K.M., Chen, K.-., Rau, R.J., and Yang, M., 2011, Modern vertical deformation rates and mountain building in Taiwan from precise leveling and continuous GPS observations, 2000–2008: Journal of Geophysical Research, v. 116.

Dadson, S.J., Hovius, N., Chen, H., et al., 2003, Links between erosion, runoff variability and seismicity in the Taiwan orogen: Nature, v. 426, p. 648-651.

Finnegan, N.J., Interpretation and downstream correlation of bedrock river terrace treads created from propagating knickpoints: Journal of Geophysical Research: Earth Surface, v. 118, p. 54-64-2013.

Finnegan, N.J., and Balco, G., 2013, Sediment supply, base level, braiding, and bedrock river terrace formation: Arroyo Seco, California, USA: Geological Society of America Bulletin.

Finnegan, N.J., and Dietrich, W.E., 2011, Episodic bedrock strath terrace formation due to meander migration and cutoff: Geology, v. 39, no. 2, p. 143-146.

Finnegan, N.J., Roe, G., Montgomery, D.R., and Hallet, B., 2004, Controls on the channel width of rivers: Implications for modeling fluvial incision of bedrock: Geology, v. 33, no. 8, p. 229-232.

Fisher, G.B., Amos, C.B., Bookhagen, B., Burbank, D.W., and Godard, V., 2012, Channel widths, landslides, faults, and beyond: The new world order of high-spatial resolution Google Earth imagery in the study of earth surface processes: Geological Society of America Special Papers, v. 492, p. 1-22.

Fisher, G.B., Bookhagen, B., and Amos, C.B., 2013, Channel planform geometry and slopes from freely available high-spatial resolution imagery and DEM fusion: Implications for channel width scalings, erosion proxies, and fl uvial signatures in tectonically active landscapes: Geomorphology, v. 194, p. 46-56.

Flint, J.J., 1974, Stream gradient as a function of order, magnitude, and discharge: Water Resources Research, v. 10, no. 5, p. 969-973.

Gourley, J.R., Byrne, T., Chan, Y.-., Wu, F., and Rau, R.-., 2007, Fault geometries illuminated from seismicity in central Taiwan: Implications for crustal scale structural boundaries in the northern Central Range: Tectonophysics, v. 445, p. 168 – 185.

Hack, J.T., 1954, Studies of longitudinal stream profiles in Virginia and Maryland: Professional Paper: 294-B.

Hartshorn, K., Hovius, N., Dade, W.B., and Slingerland, R.L., 2002, Climate-driven bedrock incision in an active mountain belt.: Science, v. 297, no. 5589, p. 2036-2038.

Ho, C.-., 1986, A synthesis of the geologic evolution of Taiwan: Tectonophysics, v. 125, no. 1-3, p. 1-16.

Howard, A.D., 1994, A detachment-limited model of drainage basin evolution: Water Resources Research, v. 30, no. 7, p. 2261-2285.

Howard, A.D., Dietrich, W.E., and Seid, M.A., 1994, Modeling fluvial erosion on regional to continental scales: Journal of Geophysical Research: Solid Earth, v. 99, no. B7, p. 13971-13986.

Howard, A.D., and Kerby, G., 1983, Channel changes in badlands: Geological Society of America Bulletin, v. 94, no. 6, p. 739-752.

Hsieh, M.-., and Capart, H., 2013, Late Holocene episodic river aggradation along the Lao-nong River (southwestern Taiwan): An application to the Tseng-wen Reservoir Transbasin Diversion Project: Engineering Geology, v. 159, p. 83–97.

Hsieh, M.L., and Knuepfer, P.L.K., 2001, Middle–late Holocene river terraces in the Erhjen River Basin, southwestern Taiwan—implications of river response to climate change and active tectonic uplift: Geomorphology, v. 38, p. 337-372.

Kirby, E., and Ouimet, W.B., 2011, Tectonic geomorphology along the eastern margin of Tibet: insights into the pattern and processes of active deformation adjacent to the Sichuan Basin: Geological Society, London, Special Publications, v. 353, p. 165-188.

Leopold, L., and Maddock, T., 1950, The hydraulic geometry of stream channels and some physiographic implications: U.S. Geological Survey Professional Paper: 252.

Leopold, L.B., Wolman, M.G., and Miller, J.P., 1995, Fluvial Processes in Geomorphology, Dover Publications, 544 p.

Liew, P., and Hsieh, M.-., 2000, Late Holocene (2 ka) sea level, river discharge and climate interrelationship in the Taiwan region: Journal of Asian Earth Sciences, v. 18, p. 499-505.

Lin, K.-., Hu, J.-., Ching, K.-., et al., 2010, GPS crustal deformation, strain rate, and seismic activity after the 1999 Chi-Chi earthquake in Taiwan: Journal of Geophysical Research, v. 115.

Montgomery, D.R., and Brandon, M.T., 2002, Topographic controls on erosion rates in tectonically active mountain ranges: Earth and Planetary Science Letters, v. 201, no. 3-4, p. 481-489.

OTA, Y., Shyu, J.B.H., Chen, Y., and HSIEH, M., 2002, Deformation and age of fluvial terraces south of the Choushui River, central Taiwan, and their tectonic implications: Western Pacific Earth Sciences, v. 2, no. 3, p. 251-260.

Ritter, D.F., Kochel, R.C., and Miller, J.R., 2011, Process Geomorphology - 5th Edition, Waveland Pr Inc.

Sklar, L., and Dietrich, W.E., 1998, River Longitudinal Profiles and Bedrock Incision Models: Stream Power and the Influence of Sediment Supply. *in* Tinkler, K.J. and Wohl, E.E., eds., Rivers Over Rock: Fluvial Processes in Bedrock Channels: Washington, D.C., USA, American Geophysical Union, p.237-260.

Snyder, N.P., Whipple, K.X., Tucker, G.E., and Merritts, D.J., 2000, Landscape response to tectonic forcing: Digital elevation model analysis of stream profiles in the Mendocino triple junction region, northern California: Geological Society of America Bulletin, v. 112, no. 8, p. 1250-1263.

Stark, C.P., Barbour, J.R., Hayakawa, Y.S., et al., 2010, The climatic signature of incised river meanders: Science, v. 327, no. 5972, p. 1497-1501.

Teng, L.S., 2000, Geotectonic evolution of late Cenozoic arc-continent collision in Taiwan: Tectonophysics, v. 183, p. 57-76.

Tucker, G.E., 2004, Drainage basin sensitivity to tectonic and climatic forcing: implications of a stochastic model for the role of entrainment and erosion thresholds: Earth Surface Processes and Landforms, v. 29, no. 2, p. 185-205.

Turowski, J.M., Hovius, N., Hsieh, M.-., Lague, D., and Chen, M.-., 2008, Distribution of erosion across bedrock channels: Earth Surface Processes and Landforms, v. 33, p. 353–363.

Whipple, K.X., and Tucker, G.E., 1999, Dynamics of the stream-power river incision model: Implications for height limits of mountain ranges, landscape response timescales, and research needs: Journal of Geophysical Research, v. 104, no. B8, p. 17661-17674.

Whipple, K.X., Wobus, C., Crosby, B., Kirby, E., and Sheehan, D., 2007, New Tools for Quantitative Ge omorphology: Extraction and Interpretation of Stream Profiles from Digital Topographic Data, GSA Annual Meeting.

Whittaker, A.C., Cowie, P.A., Attal, M., Tucker, G.E., and Roberts, G.P., 2007, Bedrock channel adjustment to tectonic forcing: Implications for predicting river incision rates: Geology, v. 35, no. 2, p. 103-106.

Willett, S.D., McCoy, S.W., Perron, J.T., Goren, L., and Chen, C.-., 2014, Dynamic Reorganization of River Basins: Science, v. 343.

Wobus, C.W., Whipple, K.X., Kirby, E., et al., 2006, Tectonics from topography: Procedures, promise, and pitfalls: GSA Special Papers, v. 398, p. 54-74.

Yanites, B.J., and Tucker, G.E., 2010, Controls and limits on bedrock channel geometry: Journal of Geophysical Research: Earth Surface, v. 115, no. F4.

Yanites, B.J., Tucker, G.E., Mueller, K.J., Chen, Y.-., Wilcox, T., Huang, S.-., and Shi, K.W., 2010, Incision and channel morphology across active structures along the Peikang River, central Taiwan: Implications for the importance of channel width: Geological Society of America Bulletin, v. 122, no. 7-8, p. 1192-1208.